SANDIA REPORT

SAND2013-5493
Unlimited Release
Printed July 2013

Evaluation of Annual Efficiencies of High Temperature Central Receiver Concentrated Solar Power Plants With Thermal Energy Storage

Brian D. Ehrhart
David D. Gill

Prepared by
Sandia National Laboratories
Albuquerque, New Mexico 87185 and Livermore, California 94550

Sandia National Laboratories is a multi-program laboratory managed and operated by Sandia Corporation, a wholly owned subsidiary of Lockheed Martin Corporation, for the U.S. Department of Energy's National Nuclear Security Administration under contract DE-AC04-94AL85000.

Issued by Sandia National Laboratories, operated for the United States Department of Energy by Sandia Corporation.

Available to DOE and DOE contractors from
U.S. Department of Energy
Office of Scientific and Technical Information
P.O. Box 62
Oak Ridge, TN 37831

Telephone: (865) 576-8401
Facsimile: (865) 576-5728
E-Mail: reports@adonis.osti.gov
Online ordering: http://www.osti.gov/bridge

Available to the public from
U.S. Department of Commerce
National Technical Information Service
5285 Port Royal Rd.
Springfield, VA 22161

Telephone: (800) 553-6847
Facsimile: (703) 605-6900
E-Mail: orders@ntis.fedworld.gov
Online order: http://www.ntis.gov/help/ordermethods.asp?loc=7-4-0#online

SAND2013-5493
Unlimited Release
Printed July 2013

Evaluation of Annual Efficiencies of High Temperature Central Receiver Concentrated Solar Power Plants With Thermal Energy Storage

Brian D. Ehrhart and David D. Gill
Concentrating Solar Technologies
Sandia National Laboratories
P.O. Box 5800
Albuquerque, NM 87185-1127

Abstract

The current study has examined four cases of a central receiver concentrated solar power plant with thermal energy storage using the DELSOL and SOLERGY computer codes. The current state-of-the-art base case was compared with a theoretical high temperature case which was based on the scaling of some input parameters and the estimation of other parameters based on performance targets from the Department of Energy SunShot Initiative. This comparison was done for both current and high temperature cases in two configurations: a surround field with an external cylindrical receiver and a north field with a single cavity receiver. There is a fairly dramatic difference between the design point and annual average performance, especially in the solar field and receiver subsystems, and also in energy losses due to the thermal energy storage being full to capacity. Additionally, there are relatively small differences (<2%) in annual average efficiencies between the Base and High Temperature cases, despite an increase in thermal to electric conversion efficiency of over 8%. This is due the increased thermal losses at higher temperature and operational losses due to subsystem start-up and shut-down. Thermal energy storage can mitigate some of these losses by utilizing larger thermal energy storage to ensure that the electric power production system does not need to stop and re-start as often, but solar energy is inherently transient. Economic and cost considerations were not considered here, but will have a significant impact on solar thermal electric power production strategy and sizing.

ACKNOWLEDGEMENTS

The authors would like to thank James E. Pacheco of Sandia National Laboratories for helpful discussions and guidance.

CONTENTS

FIGURES

TABLES

1. INTRODUCTION

1.1. Overview of Concentrated Solar Power and Central Receiver Systems

Concentrating Solar Power (CSP) focuses sunlight in order to use the heat energy of the sun. One important application of CSP is to use the heat energy of the sun to create electricity, usually at the utility scale. An advantage of CSP is the ability to store thermal energy so that the facility can match its electricity production to customer demand even when the sun is not shining. Thermal energy storage is an important technology that will enable further penetration of renewables into the electrical grid. However, the cost of CSP needs to be lower to make it fully cost-competitive with other electrical production technologies. The reduction of the cost of solar power production including CSP is the focus of the U.S. Department of Energy's SunShot Initiative.

In a central receiver system configuration, many mirrors (heliostats) individually track the sun and reflect the concentrated solar energy onto a receiver on top of a tower. The receiver contains the working fluid which is heated by the concentrated solar radiation. The working fluid can then be stored directly in insulated tanks and used to drive a power cycle to produce electric power on-demand (see Figure 1).

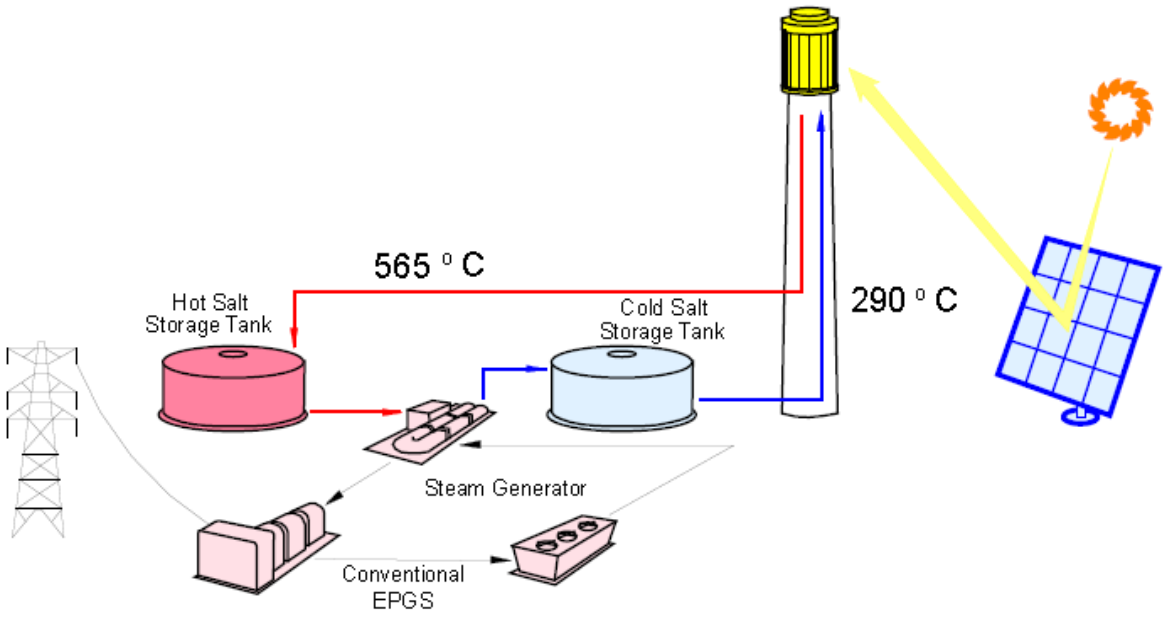

Figure 1. State-of-the-Art Molten Salt Central Receiver System (taken from [1]).

1.2. Operation at Higher Temperatures

The DOE SunShot program has a great interest in improving concentrating solar power (CSP) systems which use much higher temperatures [2-4] in order to realize higher power cycle efficiency and, hopefully, lower cost of electricity. It is therefore of interest to examine the effects that higher operating temperatures would have on the performance of both the thermal energy storage subsystem and on the overall system. The purpose of this analysis is to use real weather data to evaluate the annual efficiency of a high temperature, central receiver, concentrated solar power plant. This is done to evaluate potential higher operating temperatures for next generation central receiver plants.

The high temperature case was assumed to have an upper operating temperature of 650°C and a lower operating temperature of 250°C. This operating range is not currently available in an economical and practical sensible material, but the metrics were derived from the goals of the DOE SunShot Multi University Research Initiative [4]. Based on the temperature ranges of interest, the system is assumed to have some kind of a chloride or carbonate salt mixture, as these salts was estimated to have the best performance in terms of volumetric energy storage density and system cost [5]. However, these salts do suffer from corrosion issues at high temperatures, especially of dissolution of chromium in containment alloys; chloride salts seem unable to form passivated oxide layers, so corrosion continues to be an issue over time [6]. Chloride salts suffer when impurities such as oxygen and water are present in tank ullage gas; this effect is less significant for carbonate salts, but the chloride content of the carbonate salts lead to high corrosion [6].

1.3. Overview of DELSOL and SOLERGY Computer Codes

The DELSOL3 and SOLERGY computer codes used in this study are computer codes written in FORTRAN and developed at Sandia National Laboratories. The DELSOL3 computer code is used to calculate optimal system design and subsequent optical performance for central receiver power plants [7]. This code was used to design the PS-10 and PS-20 commercial power towers in Andalusia, Spain [1], and has been validated against other optical codes [7] and Solar Two data [8]. The SOLERGY computer code is used to calculate the annual performance of a central receiver power plant using conservation of energy [9]. SOLERGY has been validated with data from Solar One [10] and Solar Two [11]. The optical and plant designs were performed in DELSOL3 and typical meteorological year (TMY) data from Barstow, CA, was used in SOLERGY to evaluate the performance of the plant over the course of a year. The TMY data used is from The Aerospace Corporation and provides meteorological data from Barstow, CA, in the year of 1977 [12]. The SOLERGY computer code is able to use the weather data (taken at 15 minute intervals) and tracks startup, shutdown, operational mode, and performance of plant components over the course of the year. The SOLERGY code then aggregates the performance and losses for each day and the entire year.

2. PERFORMANCE ANALYSIS

2.1. General System Description

This study examines four cases of a central receiver concentrated solar power plant with sensible liquid thermal storage in Barstow, CA, that will produce 100 MW_e of gross electric power. The plant will provide 6 hours of thermal energy storage (for full rated turbine operation) and have a solar multiple of 1.8. The solar multiple is a ratio of the thermal energy input to the receiver to the thermal energy requirements of the power generation system at the design point [7]. A base case is first examined which will reflect the state-of-the-art. This is taken to be a central receiver system using a binary molten nitrate salt ($NaNO_3$-KNO_3) heat transfer fluid which drives a conventional subcritical Rankine steam cycle with dry cooling. This base case system will be primarily modeled after the subcritical dry-cooled case in [1], hereafter referred to as "Kolb 2011". The molten salt will nominally operate between 565°C and 290°C.

A High Temperature case is then compared to the base case; this high temperature case is meant to reflect a system which operates at much higher temperatures in order to drive a much more efficient power cycle. Instead of using demonstrated technologies for this case, an optimistic system will be modeled using subsystem performance goals from the DOE SunShot Initiative [2-4]. The performance goals that are included in this study are listed in Table 1 along with the associated metrics used in the base case.

Table 1. Performance Metrics for Base and High Temperature Cases.

Subsystem	Performance Metric	Base Case [1]	SunShot Goal
Receiver	Thermal Efficiency	89-90%	90% [3]
	Heat Transfer Fluid Exit Temperature	565°C	650°C [3]
Heat Transfer Fluid	Minimum Operating Temperature	290°C	250°C [4]
Thermal Storage	Efficiency	98.5%	95% [2]
Power Block	Cycle Efficiency (with dry cooling)	41.83%	50% [3]

Two different plant configurations are also examined: a surround solar field with an external cylindrical receiver, and a north solar field with a north-facing cavity receiver. The four cases to be examined in this study are then:

1. Surround Field Base Case
2. Surround Field High Temperature Case
3. North Field Base Case
4. North Field High Temperature Case

It should be noted that there is concern about the ability to operate an external solar receiver at higher temperatures and still achieve 90% thermal efficiency. While optical considerations for large scale north-fields mean that surround fields are typically more effective, it is likely that plants using a surround field at higher temperatures will take the form of something similar to a multi-cavity receiver instead of an external cylindrical receiver. The surround field with an

external cylindrical receiver is used in DELSOL and SOLERGY for simplicity but the thermal efficiency is set at 90%.

Similarly, it is noted that the SunShot performance goal for the receiver thermal efficiency of ≥90% is not much different than the current state-of-the-art value of ~89%. This is due to the fact that when operating a receiver at higher temperatures, it is much more difficult to obtain a thermal efficiency of 90% for two main reasons: higher thermal losses and changing emissivity wavelengths. The receiver will lose more heat to the ambient surroundings at higher temperature through convection and conduction, but especially through radiative losses, which are proportional to T^4. Additionally, the wavelength of radiative emissions from the receiver at the higher temperature will more closely match the wavelengths of the incoming solar radiation. Ideally, a solar receiver would have high absorptivity in the solar radiation wavelengths and low emissivity in the wavelengths at which the receiver radiates heat at its operational temperatures. However, it is very difficult to engineer materials or coatings to have high absorptivity and low emissivity in the same wavelengths. As such, the High Temperature case in this study will reflect a receiver which can operate at higher temperatures while achieving the same or slightly better relative thermal performance.

2.2. Overview of Performance Analysis Methodology

For each case, DELSOL3 is used to design the solar field, receiver dimensions, and tower height. This is done by finding the optimum design for a 100 MW_e plant based on minimization of capital cost within DELSOL3. The cost parameters are based on those found in Ref [1] and are held constant for all cases. While many of the important SunShot targets involve cost [2-4], the current study holds cost parameters constant in DELSOL and leaves the evaluation of the effect of changing cost parameters for future work. Once an optimum design is obtained, a performance calculation is done in DELSOL to calculate the optical efficiency of the solar field. The resulting optical efficiency matrix is then passed to SOLERGY along with the total heliostat mirror area of the plant design. The optical efficiency matrix from DELSOL is corrected for receiver absorptivity because this is handled separately in SOLERGY. SOLERGY then runs using these inputs, along with its own input parameters and the TMY weather file, to evaluate plant performance over the year.

2.3. Development of DELSOL and SOLERGY Input Parameters

2.3.1. Heliostat Field

The heliostat field for all cases assumes a 95 m^2 rectangular heliostat. This is similar to the ATS heliostat described in Kolb 2011 [1], and is the DELSOL default [7]. The heliostat reflectivity will be taken to be 89.3%, which is an ideal reflectivity value of 94%, and an assumed factor of cleanliness of 95%, similar to Kolb 2011 [1]. The standard deviations of optical error were set equal to the recommended parameters given in the DELSOL User's Manual, for a total standard deviation of 1.75 mrad [7]. Other parameters for the heliostats and the solar field are left at the DELSOL and SOLERGY defaults, including field spacing and error terms for blocking and shading. These values are given in Appendix A: Detailed DELSOL Inputs and Appendix C: Detailed SOLERGY Inputs for comparison.

2.3.2. Receiver

The tower height and receiver dimensions for all cases will be optimized by the DELSOL computer code. The values for these parameters in the DELSOL input are for an initial performance calculation done by DELSOL, and do not reflect the final optimized design, which is given in the output [7]. Surround field cases are designed to have a cylindrical external receiver on top of the tower; north field cases are designed to have a rectangular cavity receiver with a semi-spherical cavity inside [7]. The DELSOL computer code uses a "smart" heliostat aiming strategy, which arranges the reflected heliostat images on the receiver absorber surface roughly evenly in order to avoid flux limitations of the receiver. The external cylindrical receivers use a 1-dimensional aiming strategy along the receiver height dimension, and this is true for the entire circumference of the receiver. The rectangular cavity receivers use a 2-dimensional aiming strategy over the cavity area [7]. The receivers in all cases are assumed to have a flux limit of 1 MW/m^2, which is similar to Kolb 2011 [1], and the appropriate parameters are adjusted to ensure that these limits are met (see Appendix A: Detailed DELSOL Inputs).

Receiver Thermal Losses
Thermal losses from the solar receiver can be calculated in a variety of ways; for this study, an overall receiver thermal efficiency is assumed and the appropriate DELSOL and SOLERGY parameters are adjusted to approximate this level of performance. For all cases, a receiver efficiency of 90% is assumed; this is based both upon current state-of-the-art receiver thermal performance [1, 3] and the SunShot receiver thermal efficiency target [3].

The thermal loss of a solar receiver can be calculated from the overall thermal efficiency given by Equation 1.

$$\eta_{\mathrm{th}} = \frac{(\alpha Q_{in} - Q_{loss})}{Q_{in}} = \alpha - \frac{Q_{loss}}{Q_{in}} \qquad \textbf{Equation 1}$$

Where η_{th} is the thermal efficiency of the receiver, equal to 0.9; α is the solar absorptance of 0.94 (this value is based on Pyromark paint) [1] which is assumed to have high temperature capability for simplicity in this study, though an alternative material is likely needed at the high temperatures; Q_{in} is the incident power on receiver, and Q_{loss} is the power loss due to radiation and convection.

The power absorbed to the working fluid of the receiver (the thermal rating of the receiver in SOLERGY) is found by determining the thermal power requirements of the electric power generation system turbine and scaling this value by the solar multiple. The absorbed power (Q_{abs}) can then be used with the receiver thermal efficiency to find the incident power on the receiver, as in Equation 2.

$$Q_{abs} = \eta_{th} Q_{in} \qquad \textbf{Equation 2}$$

Once the incident and absorbed power levels have been calculated, they are used with the receiver absorptivity to calculate the thermal loss of the receiver for the specified efficiency. These calculations are summarized in Table 2.

Table 2. Power Level Calculations.

	Base Case	High Temperature Case
Gross Electric Rating	100 MW_e	100 MW_e
Turbine Efficiecy	41.83%	50%
Turbine Thermal Rating	239.06 MW_{th}	200 MW_{th}
Solar Multiple	1.8	1.8
Absorbed Power (Q_{abs})	430.31 MW_{th}	360 MW_{th}
Incident Power (Q_{in})	478.2 MW_{th}	400 MW_{th}
Thermal Loss (Q_{loss})	19.128 MW_{th}	16 MW_{th}

These loss values are then normalized per unit receiver area for comparison; these values are listed in Table 3. The thermal loss per unit area will be for the area of external receiver surface for the surround field cases. The thermal loss per unit area will be for the rectangular aperture area for the north field cases.

Table 3. Receiver Heat Loss per Unit Receiver Area.

		Surround Field		North Field	
	Thermal Loss	Receiver Area	Loss/Area	Aperture Area	Loss/Area
Base Case	19.128 MW_{th}	829.38 m^2	23.1 kW_{th}/m^2	563.55 m^2	33.9 kW_{th}/m^2
High Temp	16 MW_{th}	678.58 m^2	23.6 kW_{th}/m^2	422.71 m^2	37.9 kW_{th}/m^2

The loss per unit area values increase for the high temperature cases over the respective base cases. For the surround field cases, the loss per unit area value undergoes a 2.16% increase, while the north field loss per unit aperture area undergoes an 11.8% increase at high temperature. The values for the surround field cases especially do not seem to be a very large increase, which is counter-intuitive for a higher temperature scenario. However, the way in which these loss values were calculated does not explicitly take the higher temperature into account for the thermal losses. This was done in order to compare different receiver configurations using an optimistic technical target (90% thermal receiver efficiency at high temperature), instead of using disparate methods and assumptions to calculate thermal losses for the different cases. A possible explanation for the lower than expected increase in the loss per unit area value for the surround field cases is to assume the multi-cavity, high absorptivity, and low emissivity conditions discussed previously.

Kolb 2011 uses a surround field, so it is useful to compare thermal loss per unit area and receiver efficiency for surround field cases to Kolb 2011 values for the Base Case. The appropriate values are summarized in Table 4.

Table 4. Comparison of Surround Field Base Case to Values for the 565°C Sub-Critical Rankine Case from [1].

Case	α	Q_{abs}	Q_{loss}	Receiver Area	Loss per Unit Area	Receiver Thermal Efficiency
565°C	0.94	1000 MW_t	55.5 MW_t	1852.28 m^2	30.0 kW_{th}/m^2	89.06%
Base Case	0.94	430.31 MW_t	19.128 MW_t	829.38 m^2	23.1 kW_{th}/m^2	90.00%

The base case thermal efficiencies are similar to Kolb 2011 values (90% and 89%, respectively), whereas the loss per unit area is ~30% higher for Kolb 2011. This is due to the fact that the current method of calculating thermal losses is based on a performance metric instead of a model of the actual system. Because the assumed receiver thermal efficiency for the current study is higher than the receiver thermal efficiency in the Kolb 2011 case, the loss per unit area will subsequently be lower. The current performance metric based method of calculating thermal losses for the receiver is used in order to provide a uniform method of heat loss calculation between the four cases of the current study and to focus on the effect of innovative technical targets.

For the SOLERGY code, the receiver thermal loss while operating is a constant value, so the value of 19.128 and 16 MW_t will be used for the base cases and high temperature cases, respectively (variable PLXLR). However, the thermal losses in DELSOL are a function of receiver area so that it can be varied during optimization. Therefore, the parameters in DELSOL will need to be scaled in order to approximate the heat loss values obtained for SOLERGY. In DESOLSOL, the receiver thermal loss is given by Equation 3.

$$P_{lost,R} = Q_{rad} + Q_{conv} \qquad \textbf{Equation 3}$$

Where Q_{rad} is the radiative losses and Q_{conv} is the convective loss term. The radiative loss term is found with Equation 4.

$$Q_{rad} = \epsilon \sigma A T_{wall}^4 \qquad \textbf{Equation 4}$$

Where ϵ is the emissivity of the receiver, σ is the Stefan-Boltzmann constant, A is the aperture area of the cavity receiver, and T_{wall} is the average wall temperature of the receiver during operation at the design point. For the base case, it is left at the DELSOL default value of 753 K or 480°C, which is a weighted average temperature between the high and low operating temperatures of 565°C and 290°C (weighted average: (480-290)/(565-290) = 0.691). This value is used to obtain the radiative parameter for the DELSOL computer code [7] in Equation 5.

$$\begin{aligned} Q_{rad,base} &= (0.9)\left(5.669 \times 10^{-8} \frac{W}{m^2 K^4}\right) A (753\ K)^4 \\ &= \left(16403 \frac{\mathrm{W}}{\mathrm{m}^2}\right) \cdot A \end{aligned} \qquad \textbf{Equation 5}$$

For the high temperature case, the T_{wall} was increased to 799 K or 526°C, which is the same weighted average of the high and low temperatures 650°C and 250°C (0.691*(650-250)+250 = 526). While there are currently no heat transfer fluids that are capable of achieving this wide range of operating temperature, these values were chosen for the high temperature case based on the DOE SunShot MURI goals [4]. The parameter adjusted for the high temperature cases is shown in Equation 6. The surround field cases take the variable A to be the external cylindrical receiver surface area, whereas for the north field cavity receivers the variable A is taken to be the aperture area [7].

$$Q_{rad,\mathrm{high}} = (0.9)\left(5.669 \times 10^{-8}\frac{W}{m^2K^4}\right)A(799\ K)^4 = \left(20832\frac{\mathrm{W}}{\mathrm{m}^2}\right)\cdot A \qquad \textbf{Equation 6}$$

The convective losses for the surround field cases are given by Equation 7.

$$Q_{conv} = \mathrm{h}_{mix}A(T_{wall} - T_\infty) \qquad \textbf{Equation 7}$$

Where Q_{conv} is the power loss from convection, h_{mix} is the heat transfer coefficient of mixed (natural and forced) convection, A is the receiver surface area, T_{wall} is the same weighted average temperature as before, and T_∞ is the ambient temperature (here taken to be 20°C) [7]. Equation 8 gives the default equation for the base case.

$$Q_{conv,base} = \mathrm{h}_{mix}A\big((480°C) - (20°C)\big) = (460\ ℃)\mathrm{h}_{mix}A \qquad \textbf{Equation 8}$$

Equation 9 gives the scaled value for the high temperature case.

$$Q_{conv,\mathrm{high}} = \mathrm{h}_{mix}A\big((526°C) - (20°C)\big) = (506℃)\mathrm{h}_{mix}A \qquad \textbf{Equation 9}$$

The DELSOL parameter values entered for the Surround Field Cases (the Base Case values match the default DELSOL values) are listed in Table 5.

Table 5. DELSOL Input Parameters for Surround Field Cases.

DELSOL Parameter	Base Case	High Temp
REFRC1	16403	20832
REFRC2	460	506
REFRC3	0	0

The convective heat loss term is slightly different for cavity receivers (north field cases). In these cases, the convective heat loss is given by Equation 10.

$$Q_{conv} = Q_{forced} + Q_{nat} \qquad \textbf{Equation 10}$$

Where Q_{forced} and Q_{nat} are terms for forced and natural convection, respectively. The expressions for these loss terms (along with the default values) from DELSOL are given in Equation 11 and Equation 12.

$$Q_{forced,base} = 7631 \frac{A}{W_{ap}^{0.2}} \quad \textbf{Equation 11}$$

$$Q_{nat,base} = 5077 \cdot A_{cav} \quad \textbf{Equation 12}$$

Where A is the area of the aperture of the cavity receiver, W_{ap} is the aperture width, and A_{cav} is an approximation of the total area inside the cavity, which is given by Equation 13 [7].

$$A_{cav} = \pi \cdot (cavity\ depth) \cdot (cavity\ height) \quad \textbf{Equation 13}$$

Because both the forced and natural convection terms are proportional to the difference (T_{wall}-T_{∞}) based on Newton's law of cooling, then both of these heat loss terms will take the form $Q = C \cdot \Delta T$, where C is a constant. This is then used to scale the parameters to the higher temperatures. This relationship is shown in Equation 14.

$$Q_{forced,base} = 7631 \frac{A}{W_{ap}^{0.2}} = C_{forced}(T_{wall} - T_{\infty}) \frac{A}{W_{ap}^{0.2}} \quad \textbf{Equation 14}$$

This gives a value of C_{forced}=16.59 °C^{-1}. Then for a higher value of T_{wall} for the high temperature case, shown in Equation 15.

$$Q_{forced,high} = (16.5891\ °C^{-1})\big((526°C) - (20°C)\big) \frac{A}{W_{ap}^{0.2}} = 8400 \frac{A}{W_{ap}^{0.2}} \quad \textbf{Equation 15}$$

The natural convection term is scaled similarly in Equation 16.

$$Q_{nat,base} = 5077 \cdot A_{cav} = C_{nat}(T_{wall} - T_{\infty})A_{cav} \quad \textbf{Equation 16}$$

This results in a value of C_{nat}=11.04 °C^{-1}, which is used in Equation 17 to obtain the parameter for the high temperature case.

$$Q_{nat,high} = (11.037\ °C^{-1})\big((526°C) - (20°C)\big)A_{cav} = 5589 \cdot A_{cav} \quad \textbf{Equation 17}$$

These two values are entered into DELSOL parameters REFRC2 and REFRC3 for the north field high temperature case. The Q_{rad} parameter is the same for the north field cases and the surround field cases because DELSOL defines the receiver area differently. This gives the following DELSOL parameters for the North Field Cases in Table 6.

Table 6. DELSOL Input Parameters for North Field Cases.

DELSOL Parameter	Base Case	High Temp
REFRC1	16403	20832
REFRC2	7631	8400
REFRC3	5077	5589

The thermal efficiencies and thermal loss values for all four cases will now be calculated for comparison purposes using the resulting DELSOL receiver dimensions. To do this, Equation 3-Equation 17 are used, holding hmix constant for all cases with a value of hmix=15.015 according to the DELSOL User's Manual [7]. The resulting loss values are shown in Table 7.

Table 7. Comparison of Thermal Losses and Thermal Efficiencies for All Four Cases Based on DELSOL and SOLERGY Parameters.

		Surround Field Base Case	Surround Field High Temp	North Field Base Case	North Field High Temp
Receiver Thermal Loss	DELSOL	19.33 MW	19.30 MW	17.47 MW	15.60 MW
	SOLERGY	19.128 MW	16 MW	19.128 MW	16 MW
	Difference	1.06%	20.63%	-8.67%	-2.50%
Loss Per Unit Receiver Area	DELSOL	23.31 kW_{th}/m^2	28.43 kW_{th}/m^2	30.99 kW_{th}/m^2	36.89 kW_{th}/m^2
	SOLERGY	23.1 kW_{th}/m^2	23.6 kW_{th}/m^2	33.9 kW_{th}/m^2	37.9 kW_{th}/m^2
	Difference	0.91%	20.47%	-8.58%	-2.66%
Thermal Efficiency η_{th}	DELSOL	89.96%	89.22%	90.33%	90.10%
	SOLERGY	90%	90%	90%	90%
	Difference	-0.04%	-0.87%	0.37%	0.11%

The resulting values from DELSOL for thermal loss, loss per unit area, and thermal efficiency are shown in Table 7, along with the associated values from the previously shown values calculated for SOLERGY. A difference value of each set parameter compares the change between the DELSOL and SOLERGY values relative to the SOLERGY values. As can be seen, the values for absolute heat loss from the receiver and heat loss per unit area are relatively similar between the DELSOL and SOLERGY for most cases; the North Field Base Case have differences of <10%, and the Surround Field Base Case and North Field High Temperature Case each having differences of <3%. The notable exception is the Surround Field Base Case, which has differences for the absolute heat loss and heat loss per unit area of over 20%. This is primarily due to the ways in which the various DELSOL values were calculated; because the DELSOL parameters and loss values were calculated using estimated temperatures without changing values such as receiver emissivity, the loss for an external receiver at high temperatures will be much higher. Because this is not as much of an issue for cavity receivers, the discrepancy

is not as noticeable for the North Field cases. This highlights a major challenge for operation at higher temperatures, and a major reason why future receivers will likely need to be cavity receivers and make major advances in lowering thermal loss. However, the DELSOL values only affect the original field design slightly, as many other factors are taken into account, and the SOLERGY values are the ones used in the subsequent SOLERGY analysis, which forms the basis of this study. As such, the discrepancy in heat loss values is viewed as acceptable.

Hold Mode Thermal Loss
In SOLERGY, the receiver can also operate in a "hold" mode for 45 minutes when the insolation decreases, where the heat transfer fluid is flowing, such that the receiver can be instantly restarted if the solar insolation returns within this timeframe. As such, the receiver will also have a thermal loss associated with this mode of operation. The thermal loss will be much less, because the temperatures will not be nearly as high. These heat loss values will be estimated using a simple scaling method. Kolb 2011 uses 9 kW_{th}/m^2 for "hold mode" operation receiver thermal losses in SOLERGY [1] so the same thermal loss per unit receiver area will be used here for all four cases; these loss values are summarized in Table 8. It should be noted that the aperture area is used for cavity receiver; it is smaller than cavity area estimation, which will give a lower loss value. This is expected for cavity receivers (especially those with doors) to have lower loss values [13].

Table 8. Receiver Hold Mode Thermal Losses.

Case	Loss
Surround Field Base Case	7.46 MW
Surround Field High Temp	6.11 MW
North Field Base Case	5.07 MW
Surround Field Base Case	3.80 W

2.3.3. Storage

Thermal Losses from Piping
Thermal losses from piping in a power tower plant are minimal [7, 9]. In both DELSOL3 and SOLERGY, these losses were left at the default for the base case. For the high temperature case, they were scaled by a factor of 1.9, as this rough estimate was assumed based on the fact that the SOLERGY storage and heat exchanger thermal loss estimations for the high temperature case were roughly 1.9 times the value of the thermal losses for the base case. This simple scaling was used here because the piping losses are relatively minimal compared to other factors.

Thermal Losses from Storage
The DELSOL computer code uses a round-trip efficiency for the thermal storage subsystem when calculating the necessary thermal input required for the plant [7]. Therefore, the values for thermal storage efficiency identified in the Kolb 2011 base case and the SunShot performance

goals can be used directly. For the Base Cases, a round trip efficiency value of 98.5% will be used, which reflects the demonstrated round trip efficiency of the molten binary nitrate salt [8]. For the High Temperature Cases, an efficiency value of 95% will be used, to reflect the 95% exergetic efficiency goal in the Ref [2]. These values of 0.985 and 0.95 will therefore be entered into the DELSOL parameter EFFSTR for the Base and High Temperature cases, respectively.

The SOLERGY code uses a constant value of heat loss for the thermal energy storage subsystem rather than an efficiency value. This value will be calculated for all cases in a manner similar to that in Kolb 2011. Storage thermal losses are based on Chicago Bridge and Iron study [14], which estimated that heat loss from a 1560 MWh hot tank was 244 kW. Thermal losses for the associated cold tank were not given, but can be estimated by assuming the same overall heat transfer coefficient as the hot tank in Equation 18.

$$Q_{hot} = U * \Delta T_{hot} \quad \Rightarrow \quad U = \frac{Q_{hot}}{\Delta T_{hot}} = \frac{244\ \text{kW}}{565°\text{C} - 25°\text{C}} = 0.45\frac{\text{kW}}{°\text{C}} \qquad \textbf{Equation 18}$$

The same scaling factor is used for the cold tank in Equation 19 .

$$Q_{cold} = U * \Delta T_{cold} = \left(0.45\frac{\text{kW}}{°\text{C}}\right)(290°\text{C} - 25°\text{C}) = 119\ \text{kW} \qquad \textbf{Equation 19}$$

Then the total storage losses for the study are approximately 244 kW + 119 kW = 363 kW for a 1560 MWh system. This gives an approximation for the total storage thermal losses per unit storage system size for the base case (denoted here as $C_{store,base}$), which is shown in Equation 20.

$$C_{store,base} = \frac{363\ \text{kW}}{1560\ \text{MWh}} = 0.233\frac{\text{kW}}{\text{MWh}} \qquad \textbf{Equation 20}$$

Because the base case has 1434 MWh of storage, then the total losses for the base case are: 0.23*1434 = 330 kW. This will be entered into the SOLERGY storage thermal loss parameter TNKLF for the base cases.

The high temperature case will be scaled for different operational temperatures. To scale the original system study given in Ref. [14] to higher temperature, the same overall heat transfer coefficient will be used, along with heat transfer fluid temperatures taken from the SunShot performance goals. This is shown in Equation 21.

$$Q_{total} = Q_{hot} + Q_{cold} = \left(0.45\frac{\text{kW}}{°\text{C}}\right)\left((650°\text{C} - 25°\text{C}) + (250°\text{C} - 25°\text{C})\right) = 850\ \text{kW} \qquad \textbf{Equation 21}$$

This gives a modified heat loss expression for the 1560 MWh system, meaning that the approximate storage heat loss per unit storage size is now given by $C_{store,high}$ in Equation 22.

$$C_{store,high} = \frac{850\ \text{kW}}{1560\ \text{MWh}} = 0.545\,\frac{\text{kW}}{\text{MWh}}$$ **Equation 22**

For the high temperature case, the storage system size is 1200 MWh, meaning the storage heat loss for the high temperature case is approximately 0.545*1200 = 654 kW. This will be entered into the SOLERGY storage thermal loss parameter TNKLF for the high temperature cases.

2.3.4. Electricity Generation System

Heat Exchanger Heat Losses
The Kolb 2011 study assumed that the steam generator will operate with similar losses to the storage system [1]. The SOLERGY code uses a constant value for heat loss from storage (in MW), and a constant value of heat loss from the steam generator while it is operating; Kolb 2011 set the value for heat loss from the steam generator equal to the value for heat loss from storage [1]. The same assumption is made in this study for both the base and high temperature cases. While it is unknown what type of power cycle will be operated at this scale and at these operational temperatures for the high temperature case, it is assumed that some type of heat exchanger will be used to transfer heat from storage to the power cycle, and that this heat exchanger will have losses similar to the storage system.

The dispatch strategy in SOLERGY is taken to be a "sun-following" strategy; that is, electricity will be produced whenever there is enough energy to do so. The turbine will start up as soon as enough energy is being delivered to an operational receiver, and will continue to be produced until there is not enough available energy either from the receiver or from thermal storage [9]. This is the default dispatch strategy in SOLERGY, and also used in Kolb 2011 [1, 9]. While the economic value of the electricity produced can be greatly increased using thermal storage to produce electricity when it is most profitable, that is not considered here as electricity pricing is unique to every power purchase agreement and every power purchasing utility.

Turbine Efficiency
The DOE SunShot goal for high temperature, dry-cooled power cycle efficiency is ≥50%, this value is used for the high temperature case turbine efficiency [3]. The DELSOL3 and SOLERGY default values of turbine efficiency (41.83%) were used for the base case [7, 9], which is the value for a Rankine cycle with a dry-cooled condenser [1]. In DELSOL3, the turbine efficiency is a single value for the design point power level [7]. In SOLERGY, the design point turbine efficiency was de-rated to account for somewhat lower efficiencies during sub-rated operation of the turbine (e.g., during turbine startup) [9]. The default de-rating in SOLERGY was scaled to the higher design point efficiency, as shown in Table 9 and Table 10.

Table 9. Turbine Efficiency Scaling for the Base Case.

Fraction of Rated Load	Turbine Efficiency [1]	Fraction of Design Point Efficiency (calculated)
0.2907	0.3598	0.8601
0.5239	0.3992	0.9543
0.7563	0.4148	0.9916
1.0	0.4183	1.0

Table 10. Turbine Efficiency Scaling for the High Temperature Case.

Fraction of Rated Load	Fraction of Design Point Efficiency (from above)	Turbine Efficiency (calculated)
0.2907	0.8601	0.4301
0.5239	0.9543	0.4772
0.7563	0.9916	0.4958
1.0	1.0	0.5

These values for turbine efficiency will be used in the SOLERGY parameter FEPSS for the indicated Fractions of Rated Load.

2.3.5. Electric Parasitics

This section describes parameters in SOLERGY that calculate and account for the various electrical parasitic loads in the CSP plant. This section of the SOLERGY code was not included in the original version, and thus is not listed or described in [9], but is described in a later report [15]. These electrical parasitics are taken out after the gross power (100 MW_e in this study) has been produced by the electric power generation system.

Many of the input parameter values were taken directly from the Kolb 2011 report, including the power to run the heliostat field per unit mirror area, the number of time steps in receiver hold mode, and baseline parasitics for forced and scheduled outages [1]. These parameters were held constant for all four cases considered here. The input parameters for the cold salt pump were taken from the Kolb 2011 dry-cooled sub-critical case, and kept constant for all four cases here. This was done because the low temperature will likely be similar for all 4 cases, estimated at 290°C and 250°C for the base and high temperature cases, respectively. The cold pump parasitic load is calculated using Equation 23, in which *w* is the fraction of full receiver flow and C1, C2, and C3 are input parameters PA(3), PA(4), and PA(5), respectively [1].

$$P_{cold\ pump} = C_1 + C_2 \cdot w + C_3 \cdot w^2 \qquad \textbf{Equation 23}$$

Some of the values were not listed in the Kolb 2011 study, and others were different than the meaning explained in the Kolb 2011 study, the different meanings were outlined in Ref [15]. The

power required to stow the heliostat field, PG&E Cooler parameters, and shutdown load were left at the default values listed in [15] for all cases. The PG&E cooler is for a dry-cooled system, which is well aligned with current technology and future technical goals due to water restriction in the arid locations in which CSP plant are located [3], whereas the electric parasitic model used in the Kolb 2011 considered the dry-cooling cases a slightly different way [1].

The parasitic load for the hot salt pump were estimated in the Kolb 2011 report through scaling a calculation done in a Babcock and Wilcox U.S. Utility Study [1]. The parasitic load will be estimated in the same way here. The Utility Study found that the hot salt pumps consumed 660 kW_e in order to supply enough hot salt to run a 260 MW_t steam generator. The Kolb 2011 report linearly scaled this value in order to match the steam generator thermal rating [1], and this study will do the same. The scaling factor is given in the first row of Table 11. This is then scaled to the turbine subsystem thermal rating for the base and high temperature cases; the calculations are done in the second two rows of Table 11.

Table 11. Scaling of Hot Salt Pump Parasitic Load.

Scaling Factor:	$\frac{660\ kW_e}{260\ MW_t} = 2.5385 \frac{kW_e}{MW_t}$
Base Cases:	$239\ MW_t \cdot 2.5385 \frac{kW_e}{MW_t} = 606.7\ kW_e$
High Temperature Cases:	$20\ MW_t \cdot 2.5385 \frac{kW_e}{MW_t} = 507.7\ kW_e$

The parasitic load of the electric power generating system plant itself is estimated as a function of power production level in the Kolb 2011, and a modified version of this estimation is used here. For the Base Cases in the current study, the curve from the sub-critical dry-cooled Kolb 2011 case is used, and for the high temperature cases in the current study, the curve from the ultra-supercritical dry-cooling case from Kolb 2011 is used. This was done because the sub-critical dry-cooled Kolb 2011 case is for a molten salt tower with an external cylindrical receiver operating between 565°C and 290°C; this matches the current base cases very well, albeit they are for a surround field and not a north field [1]. However, both of the equations from Kolb 2011 include a term with the dry bulb temperature [1], whereas in the current study the dry cooling is handled using other parameters (as described above). Therefore this term is dropped from the fitted equation in Kolb 2011, and the resulting equation is used here. These modified equations are shown in Table 12, and the values correspond to SOLERGY input parameters PA(7) and PA(8), for the constant and linear scaling value in Table 12respectively.

Table 12. Modified Electric Power Generating System Plant Parasitic Load Equations.

Base Case	$P_{plant} = -1.0404 + 3.6395 \cdot \text{ PL}$
High Temperature Case	$P_{plant} = -0.8861 + 7.2406 \cdot \text{ PL}$

All of the input parameters detailed above are outlined in Appendix A: Detailed DELSOL Inputs and Appendix C: Detailed SOLERGY Inputs.

This page intentionally left blank.

3. RESULTS

3.1. DELSOL Plant Design Results

A summary of results from DELSOL are given in Table 13.

Table 13. Summary of DELSOL Optimized System Design Results.

	Surround Field – Base Case	Surround Field – High Temperature Case	North Field – Base Case	North Field – High Temperature Case
Tower Height	177.63 m	160.53 m	263.16 m	228.95 m
Receiver Dimensions	12.0 m (D) x 22.0 m (H)	12.0 m (D) x 18.0 m (H)	Aperture: 20.56 m (W) x 27.41 m (H) Cavity: 12.22 m (D) x 30.15 m (H)	Aperture: 20.56 m (W) x 20.56 m (H) Cavity: 12.22 m (D) x 22.61 m (H)
Number of Heliostats	9618	8282	9093	8099
Land Use	5.956 km^2	5.347 km^2	5.544 km^2	5.215 km^2

These DELSOL results show one of the chief values of achieving the higher efficiency goals of the SunShot program. The solar field, which often accounts for 50% of the capital cost of a CSP plant [16], is significantly reduced in size. Any cost reductions to the field could have a significant effect on the overall electricity cost for CSP. The above values reflect a 13.9% and a 10.9% decrease in the number of heliostats required for going from the Base to the High Temperature case for the surround field and north field, respectively.

3.2. SOLERGY Plant Performance Results

A summary of results from SOLERGY for all four cases is shown in Table 14.

Table 14. Summary of Subsystem and Overall Efficiencies from SOLERGY Results.

	Surround Field – Base Case		Surround Field – High Temperature Case		North Field – Base Case		North Field – High Temperature Case	
Subsystem	Design Point	Annual	Design Point	Annual	Design Point	Annual	Design Point	Annual
Field	0.63689	0.56151	0.63955	0.56398	0.66959	0.56548	0.64281	0.54452
Storage Full	N/A	0.949	N/A	0.944	N/A	0.964	N/A	0.960
Receiver	0.89998	0.78560	0.90000	0.77256	0.89998	0.79691	0.90000	0.78945
Piping	0.99970	0.99961	0.99943	0.99927	0.99970	0.99961	0.99943	0.99926
Thermal Storage	N/A	0.99575	N/A	0.99012	N/A	0.99570	N/A	0.98998
Power Block	0.41830	0.40982	0.50000	0.49015	0.41830	0.40961	0.50000	0.48983
Parasitics	N/A	0.828	N/A	0.792	N/A	0.828	N/A	0.792
Overall	N/A	0.14131	N/A	0.15795	N/A	0.14667	N/A	0.15833

The capacity factor is a useful metric for comparing the availability of a power source, so this will be calculated from the SOLERGY output. The capacity factor is a ratio of the total electric power produced to the amount of electric power produced if the generator was running at full capacity all the time. The equation used to calculate the capacity factor for each case is shown in Equation 24.

$$CF = \frac{W_{gross}}{\left(365\ days \times 24 \frac{hours}{day}\right) W_{turbine}}$$ **Equation 24**

In Equation 24, CF is the capacity factor, W_{gross} is the gross electric power produced over the course of the year (from SOLERGY output), and $W_{turbine}$ is the design point electric power rating of the electric power generating system. The results of these calculations, along with the dry-cooled subcritical 565°C case from Kolb 2011, are displayed in Table 15.

Table 15. Summary of Capacity Factors.

Case	Capacity Factor
Kolb 2011 Dry-Cooled Subcritical Case [1]	73.7%
Surround Field – Base Case	48.5%
Surround Field – High Temperature Case	48.8%
North Field – Base Case	47.5%
North Field – High Temperature Case	47.8%

4. DISCUSSION

4.1. Comparison of Base Case to Previous Study

The first comparison will be to examine the performance differences between the Surround Field Base Case in the current study and the subcritical plant with dry cooling from the Kolb 2011 study. A summary of the annual efficiencies for both of these cases is shown in Table 16. In the following discussions, the loss terms from the SOLERGY output are listed in Appendix D: Annual Summaries from SOLERGY.

Table 16. Annual Efficiencies for Current Study Surround Field Base Case Comparison to Kolb 2011 Sub-Critical Rankine Case.

Subsystem	Current Study SF-BC	Kolb 2011 [1]
Field	0.562	0.522
Storage Full	0.949	0.951
Receiver	0.786	0.858
Piping	1.000	1.000
Thermal Storage	0.996	0.993
Power Block	0.410	0.415
Parasitics	0.828	0.915
Overall	0.141	0.160

The Kolb 2011 losses for the solar field are lower due to the way in which thermal losses due to receiver absorbance are calculated in SOLERGY. When the solar field optical efficiency matrix is calculated in DELSOL, it includes the receiver absorptivity; this effect can be removed from the matrix before entering it into SOLERGY in order to account for receiver absorptivity separately in the SOLERGY receiver calculations. The current study took this approach, whereas the Kolb 2011 study left the receiver absorptivity in the solar field optical efficiency matrix, meaning that this loss was accounted for in the Solar Field section rather than the Receiver section. However, there is a difference between the overall heliostat field efficiency (cosine, shadowing, blocking, spillage, transmission, and operation limits) between the two cases. The current study loses 43.85% of the available energy to these losses, while Kolb 2011 loses 47.03%. This is primarily due to the larger scale of the Kolb 2011 system; each additional heliostat added is further away from the tower, increasing all of the previously listed losses and making it much less effective. This brings the overall field efficiency down for larger systems; this is a well-known trade-off that must be considered when making designs about system size.

There are two main reasons for the difference in receiver annual efficiency between the current and Kolb 2011 studies: the previously discussed receiver absorbance calculation and surplus energy to the receiver. The second largest source of annual heat loss for the receiver in the current study is the surplus energy to the receiver (SOLERGY variable YSPTR), which is when the heliostats must defocus because there is more energy going to the receiver than it is rated to withstand. The current study loses 5.48% of the receiver incident energy over the course of the year to this effect, whereas the Kolb 2011 study only loses 0.47%. A receiver with a higher

thermal rating, such as the one in the Kolb 2011 study, is able to utilize more of the heat that is collected by the solar field due to the fact that heliostats do not have to defocus as often to avoid overloading the receiver. In this way, the receiver is able to absorb power from a much wider range of insolation levels. This makes the receiver much more efficient on an annual basis and contributes to the large differences in plant capacity factor between Kolb 2011 and the current study. Other receiver losses are fairly similar between the Kolb 2011 and the current study. This includes the receiver minimum flow loss, where the amount of energy is too small for the receiver to realistically flow heat transfer fluid and so enters hold mode. Also similar is the receiver startup loss, which is the loss in energy incurred when the receiver is in startup mode and therefore not able to collect useful energy. In both of these cases, the relative loss is slightly higher for the Kolb 2011 case, due to the fact that the receiver is a larger scale than the current study; as stated previously, the current study has a solar multiple of 1.8, while the Kolb 2011 study has a solar multiple of 3.0. Lastly, the percentage thermal losses between the studies are similar, though slightly larger for the Kolb 2011 study (6.97% of receiver incident energy for Kolb 2011, as opposed to 4.77% for the current study); this is due to the slightly more thermally efficiency receiver in the current study, as discussed above.

When the thermal storage system is fully charged but the receiver is still collecting excess energy, it must defocus heliostats away from the receiver as there is nowhere for the excess energy in the receiver to go. This results in a loss, as the energy collected by the defocused heliostats is wasted; this loss is reflected in the "Storage Full" (SOLERGY variable YSUPTR) line of the SOLERGY output. These loss factors are similar for both cases relative to system size; the current study loses 5.13% of the energy from the field over the course of the year, and the Kolb 2011 study loses 4.93% of the energy from the field. The Kolb 2011 study has somewhat lower YSUPTR losses due to the fact that that the Kolb 2011 system has a much larger thermal energy storage subsystem, as it is sized for 15 hours of storage, rather than the 6 hours of storage of the current study. This also results in a much higher capacity factor, as can be seen in Table 15.

Both the current study and Kolb 2011 have very small losses from piping relative to system size, both of which amount to 0.04% of the receiver absorbed energy. The direct molten salt storage for both the current Surround Field Base Case and the Kolb 2011 case means that the storage subsystem will have a very high efficiency. The current study has slightly less heat loss from storage compared to the Kolb 2011 study; the current study loses 0.28% of the energy to storage due to heat loss from the tank, while the Kolb 2011 study loses 0.40%. This is due to the fact that the current study has a smaller (6 hour) storage system than the Kolb 2011 (15 hour) storage system. Additionally, the heat loss from the steam generator relative to the energy to storage is slightly larger for the Kolb 2011 study over the current study (0.30% for Kolb 2011 and 0.15% for the current study). Again, this is due to the larger scale of the Kolb 2011 study. As was previously mentioned, both of these effects are very small relative to the system size.

The electric power generation system is very similar for both the current and Kolb 2011 study. The Rankine loss is the energy lost in the conversion from thermal to electric energy. Both of these are very similar, as the thermal-to-electric efficiency is very similar for both cases. The turbine sync loss shows a more significant change; the current study loses 1.91% of the energy to the turbine, while Kolb 2011 only loses 0.73%. This is another effect of the larger scale system;

with a larger receiver collecting more energy for a larger thermal storage system, the turbine does not have to stop and start as many times, leading to less energy lost to turbine sync. However, this turbine sync loss is relatively small (<2% of the energy to the turbine for both cases) and so does not have a very substantial effect on overall annual efficiency.

The total losses from electric parasitics (also called Auxiliary Energy in SOLERGY) are fairly similar in an absolute sense between the current and Kolb 2011 studies: the SOLERGY variable YPARN is 73091.05 MWh_e for the current study and 75868.24 MWh_e for the Kolb 2011 study. However, this does lead to a difference in the fractional losses between the two cases, because the parasitics are a smaller fraction of the larger scale Kolb 2011 electricity production. This again demonstrates the benefits of economies of scale when operating a larger plant.

4.2. Comparison of Base and High Temperature Cases

The differences between the Base Cases and the High Temperatures cases in the current study will be examined. The solar field contributes a large loss to system efficiency. Generally the losses are from the optical efficiency of the field, both in terms of reflectivity but also sun position; when the sun is low in the sky, the solar field will be less efficient. While the solar field losses do make up a significant efficiency drop, there are very few differences between the four cases in the losses from the solar field, at least on a relative basis. Most every case loses approximately 43.6% of the available energy in the solar field; the North Field High Temperature case loses slightly more, at 45.55%. This is due to the relatively lower field optical efficiency for that case (see Appendix B: Additional DELSOL Outputs), which stems from the fact that a cavity receiver will have higher spillage losses from the edges of the reflected solar image hitting the external sides of the aperture instead of passing through and being absorbed by the working fluid. This is especially true when the reflected solar image is not very round, such as the early morning or late evening.

The losses from heliostat defocusing due to the thermal storage being full is very similar for all four cases because they all have 6 hours of thermal storage. There is a very small increase in the fractional loss between the Base and High Temperature cases for both the surround and north fields (5.13% to 5.57% for surround field cases, and 3.58% to 4.00% for the north field cases), while the absolute loss decreases. This is due to the smaller thermal scale of the high temperature cases, leading to a higher relative loss.

Receiver losses are fairly similar for all four cases due to the fact that thermal losses were calculated such that the receiver thermal efficiency would be 90% for each case. The specific relative loss terms only vary from each other by approximately 1% or less between the Base and High Temperature cases. Additionally, the Surround and North Field cases only differ by approximately 1% when comparing the relative losses because, aside from the thermal losses, there is very little difference in terms of receiver operational losses, such as start-up or shut-down, as these parameters were very similar between all four cases.

The piping losses relative to the receiver absorbed energy increase between the Base and High Temperature cases from a 0.04% loss to 0.07%; this effect is the same for both the Surround

Field and North Field cases. This is due to the direct scaling that was done to the input parameters; as discussed previously, this effect is very small.

The heat losses from the storage tank increase between the Base and High Temperature cases from 0.28% to 0.65% relative to the energy put into storage. Additionally, the heat losses from the steam generator increase similarly from 0.15% to 0.34% between the Base and High Temperature cases. These effects are seen in both the Surround and North Field cases. The heat losses from storage are higher for the High Temperature cases than for the Base cases, but the overall effect is still very small.

There is an obvious effect on turbine efficiency when comparing the Base Case to the High Temperature Case for both the Surround and North Field cases; the higher turbine efficiency used for the High Temperature case leads to much less loss for electricity production. The turbine sync loss is relatively unchanged between the four cases, at just under 2% of the energy to the turbine. There is a very slight (<0.1%) decrease in the High Temperature case compared to the Base Case, but this effect is small.

There is a moderate increase in the electrical parasitic loss between the Base and High Temperature cases for both the Surround and North Field cases. Many of the individual sources of parasitic load are relatively the same (differing by <0.1%), but the parasitic load of the turbine plant relative to the gross electric power produced is 6.83% for the High Temperature Cases while only 3.17% for the Base Cases. This is due to the higher turbine plant parasitics assumed for the higher temperature and higher thermal-to-electric efficiency turbine. This leads to an increase in the total parasitic load relative to the gross electricity produced from 17.23% for the Surround Field Base Case to 20.84% for the Surround Field High Temperature case (there is a similar increase for the North Field cases). However, this ~3% difference is somewhat less than other losses because it is relative to the gross electric power produced, and not the input thermal energy in the plant.

As can be seen from the overall efficiencies, the increase in annual efficiency is fairly small between the Base and High Temperature cases for both the Surround and North Field cases. Even without the increase in electrical parasitic load between the Base and High Temperature cases, the increase on an annual basis is ~2%. The annual solar-to-electric efficiency was calculated with and without the electric parasitics, and is shown in Table 17. This was done by simply dividing the Gross Energy Output and Net Energy Output each by the Total Insolation to find the efficiency with and without parasitics, respectively.

Table 17. Solar to Electric Annual Efficiencies with and without Parasitic Electrical Loads.

	Solar to Electric Annual Efficiency, Gross	Solar to Electric Annual Efficiency, Net
Surround Field Base Case	17.07%	14.13%
Surround Field High Temperature Case	19.95%	15.79%
North Field Base Case	17.71%	14.67%
North Field High Temperature Case	20.00%	15.83%

Surround field and north field results are very similar, especially on a relative basis. As discussed above, there are a number of trade-offs between a surround and north field; a larger north field system needs to place heliostats much further away from the tower, but the cavity receiver typically has much less heat loss compared to an cylindrical external receiver. In the current study the overall annual system performance is slightly better for the North Field cases, with the annual efficiency improving by 0.5% for the Base Cases and 0.05% for the high temperature cases. Again, this similarity in performance is likely due to the fact that the receiver thermal losses were set at a particular performance level, which may be difficult to achieve at higher temperatures. It is important to consider that in the high temp case, the receiver efficiency was fixed at the SunShot target, so the surround field case is very likely a multitude of cavity receivers or some other innovative design and not a cylindrical open receiver as is currently typical on surround field systems.

Lastly, it must be noted that the current study assumed that the high temperature case would utilize a sensible liquid similar to a molten salt system. While research is ongoing to develop molten salt formulations that can reach high enough temperatures to match the SunShot performance targets, there are many other research projects that are examining latent, thermochemical, and solid sensible heat storage. This means that some of the implicit or explicit assumptions made here would not necessarily hold. Mostly this will affect the DELSOL optical designing of the receiver, in which the molten salt assumption comes to bear on many design designs within the code. However, aside from the north and surround field differences described above, there are many other design considerations that still hold true in the DELSOL code. For example, the design and spacing the solar field is likely to continue to follow similar principles, though the design and cost of heliostats may change. The SOLERGY code uses energy flows within the plant, and so does not explicitly assume a particular kind of heat transfer fluid or mechanism. That said, many of the input parameters in the current study assumed a molten salt-type system, such as the electric parasitics from the hot and cold salt pumps. However, this is held as an acceptable assumption, due to the fact that some sort of parasitic will be required to move mass or energy within the system.

Additionally, the current study uses a direct storage system, whereby the heat transfer fluid is directly stored in the thermal energy storage subsystem without the use of a secondary head exchanger between the receiver and storage subsystems. Depending on future developments in receiver and thermal storage technology, additional heat exchangers may be needed here or

elsewhere in the system; these heat exchangers will necessarily impose an efficiency loss on the thermal energy transferred, lowering the overall system efficiency further. Additionally, as is seen in the current study, the startup times for the receiver and steam generator imposed additional energy penalties which lead to discarded heat; additional heat exchangers will increase this effect. These transient effects are a major source of loss in the current study, and will continue to be a major concern for transient renewable energy.

5. CONCLUSION

The current study has examined four cases of a central receiver concentrated solar power plant with thermal energy storage using the DELSOL and SOLERGY computer codes. The differences between a current state-of-the-art base case was compared with a theoretical high temperature case, which was based on the scaling of some input parameters and the estimation of other parameters using the performance targets from the Department of Energy SunShot Initiative. This comparison was done for both a surround field with an external cylindrical receiver and a north field with a single cavity receiver. The optical designs for all four cases were done using the DELSOL computer code; the results were then passed to the SOLERGY computer code which uses historical typical meteorological year (TMY) data to estimate the plant performance over the course of one year of operation. The methodology of using DELSOL and SOLERGY followed a previous study closely and the appropriate Surround Field Base Case was benchmarked and compared to this previous study. The results of the SOLERGY simulation were then analyzed and compared between the four cases.

Each of the four cases was sized to produce 100 MW_e of gross electric power, have thermal storage capacity to generate electric power at full rated production level for 6 hours, and have a solar multiple of 1.8, which is the ratio of the thermal energy to the solar receiver from the heliostat field to the thermal energy required by the electric power generation system. This led to various system sizes for the four cases, primarily due to the increase in electric power generation system efficiency for the High Temperature cases yielding a smaller thermal system because less thermal energy is needed to generate the same amount of electricity. The High Temperature cases were estimated to have higher thermal energy losses throughout the system though these were mitigated somewhat by the smaller system scale.

One notable conclusion is the fairly dramatic difference between the design point and annual average performance. Differences between design point and annual average performance for individual cases are outlined in Table 14. The largest differences are in the solar field and receiver subsystems and also in energy losses from the thermal energy storage being full to capacity. The losses in the solar field are generally due to sub-optimal sun position which changes throughout the day and year. These differences between the design point and annual average efficiency values are typically due to losses incurred while system components are starting up and shutting down, especially in the receiver subsystem. Additional losses in the receiver subsystem are from more power being sent to the receiver than its input rating, necessitating heliostats to defocus and discard their energy in order to not damage system components. Lastly, energy is discarded when excess energy is input to the receiver while the thermal energy subsystem is full due to defocusing heliostats. Some of these losses can be mitigated by increased system size, but transient effects are inherent to solar energy.

A notable finding in the current study is the relatively small difference in annual average efficiencies between the Base and High Temperature cases. For both the Surround Field and North Field cases, the increase in annual solar to electric efficiency is <2%. This is despite an increase in thermal to electric conversion efficiency of over 8%. The reasons for this include the increased thermal losses due to higher temperature operation and operational losses due to start-

up and shut-down of plant sub-systems. The thermal losses were estimated using optimistic (not currently achievable) technical performance targets, so the current study could even over-predict the performance of high temperature operation in a real system. The operational losses are a major source of loss for the system as a whole, and are due to the transient nature of solar power. These losses are part of the nature of solar power and are subsequently difficult to overcome. Thermal energy storage can mitigate some of these losses by ensuring that the electric power production system does not need to stop and re-start as often, but additional storage brings additional capital costs and must be justified through techno-economic analyses and favorable power purchase agreements. However, the losses from these transient conditions emphasize why a plant might be constructed with significant thermal storage even if the power purchase agreement did not incentivize use of storage.

An important consideration to the current study was the fact that a sensible liquid molten salt direct storage system was assumed for both the Base and High Temperature cases. While potential higher temperature systems may not use molten salt as a heat transfer fluid or thermal storage media, analogous system components are expected. It is expected that any future system will need some way to move heat around the system which will incur a parasitic load of some kind and be analogous to the hot and cold salt pumps used in the current system. Additionally, it is expected that some sort of heat exchanger will be necessary to provide heat to the electric power generation system, which will be analogous to the steam generator used here. An important consideration is that if future systems do not match heat transfer fluid with storage media, additional heat exchangers in the system will incur increased losses which will further degrade system performance both in design point operation and annual average performance.

Lastly, it is notable that the current study only considers thermal and electric system performance, while many of the SunShot Initiative targets include goals for system and component cost. Cost is not considered in the current study, but will have a major effect on the cost of solar energy because capital cost of the plant is obviously a major consideration for solar thermal power plants.

6. REFERENCES

1. Kolb, G.J., An Evaluation of Possible Next-Generation High-Temperature Molten-Salt Power Towers, 2011, Sandia National Laboratories: Albuquerque, NM.
2. High Energy Advanced Thermal Storage (HEATS) Funding Opportunity Announcement, Advanced Research Projects Agency (ARPA-E) Department of Energy, Editor 2011.
3. SunShot Concentrating Solar Power (CSP) R&D Funding Opportunity Announcement, Department of Energy, Editor 2011: Golden, CO.
4. Multidisciplinary University Research Initiative: High Operating Temperature Fluids Funding Opportunity Announcement (MURI: HOT Fluids), Department of Energy, Editor 2012: Golden, CO.
5. Wu, Y.-t., et al., Experimental study on optimized composition of mixed carbonate salt for sensible heat storage in solar thermal power plant. Solar Energy, 2011. 85(9): p. 1957-1966.
6. Kruizenga, A.M., Corrosion Mechanisms in Chloride and Carbonate Salts, 2012, Sandia National Laboratories: Livermore, CA.
7. Kistler, B.L., A User's Manual for DELSOL3: A Computer Code for Calculating the Optical Performance and Optimal System Design for Solar Thermal Central Receiver Plants, 1986, Sandia National Laboratories.
8. Pacheco (Editor), J.E., et al., Final Test and Evaluation Results from the Solar Two Project, 2002, Sandia National Laboratories.
9. Stoddard, M.C., et al., SOLERGY - A Computer Code for Calculating the Annual Energy from Central Receiver Power Plants, 1987, Sandia National Laboratories.
10. Alpert, D.J. and G.J. Kolb, Performance of the Solar One Power Plant as Simulated by the SOLERGY Computer Code, 1988, Sandia National Laboratories: Albuquerque, NM.
11. Reilly, H.E. and G.J. Kolb, An Evaluation of Molten-Salt Power Towers Including Results of the Solar Two Project, 2001, Sandia National Laboratories: Albuquerque, NM.
12. Randall, C.M., Barstow Insolation and Meteorological Data Base, 1978, The Aerospace Corporation: El Segundo, CA.
13. Falcone, P.K., Handbook for solar central receiver design, 1986, Sandia National Laboratories: Livermore, CA.
14. Bechtel Coporation, Investigation of Thermal Storage and Steam Generator Issues, 1993, Sandia National Laboratories.
15. Chavez, J.M., G.J. Kolb, and W. Meinecke, Second Generation Central Receiver Technologies: A Status Report1993.
16. Kolb, G.J., et al., Heliostat Cost Reduction Study, 2007, Sandia National Laboratories.

This page intentionally left blank.

APPENDIX A: DETAILED DELSOL INPUTS

Variable	Description	Surround Field – Base Case	Surround Field – High Temp	North Field – Base Case	North Field – High Temp
BASIC					
IPROB	Type of Performance Calculation (=4 for design/optimization, =3 for AZ-EL Calculation for SOLERGY)	4,3	4,3	4,3	4,3
NYEAR	Number of days in the half year used in initial performance calculation	5	5	5	5
HRDEL	Time step, in hours	1	1	1	1
UDAY	Day of the year for performance calculation when IPROB=1 or 2	81	81	81	81
UTIME	Hours past solar noon for performance calculation when IPROB=2	0	0	0	0
NUAZ NUEL UAZ UEL	Sun angles for performance calculation when IPROB=3 (to generate optical efficiency matrix)	7 6 0, 30, 60, 75, 90, 110, 130 0.5, 25, 45, 65, 75, 85	7 6 0, 30, 60, 75, 90, 110, 130 0.5, 25, 45, 65, 75, 85	7 6 0, 30, 60, 75, 90, 110, 130 0.5, 25, 45, 65, 75, 85	7 6 0, 30, 60, 75, 90, 110, 130 0.5, 25, 45, 65, 75, 85
DHOPT	Density and aspect ratio variance range for heliostat optimization	0.2	0.2	0.2	0.2
IPRINT	Control parameter to print zone by zone output of performance calc. the annual zone by zone performance is always printed	9'0	9'0	9'0	9'0
ITAPE	Control panel for reading and writing file =0 no reading/writing =1 output of performance run written to Unit 10 =3 read from Unit 10	1,3	1,3	1,3	1,3
TDESP	Power level (MW) of optimized system to be rerun (if ITAPE=3)	100	100	100	100
PLAT	Latitude in degrees of solar plant location	35	35	35	35
ALT	Altitude, in km, of solar plant location	0.65	0.65	0.65	0.65
INSOL	Insolation vs time model =0 Meinel model, value for ALT required	0	0	0	0
SOLCON	Value of constant insolation kw/m2, used with INSOL=2	0.95	0.95	0.95	0.95
IWEATH	Site dependent weather factors	0	0	0	0
WEATH	Uniform cloudiness factor	0.83	0.83	0.83	0.83
H2O PRES	Mm of precipitable water in atmosphere, PRES is constant pressure relative to sea level	20 1.0	20 1.0	20 1.0	20 1.0
NSUN	Control parameter for sunshape model =0 point sun =1 limb darkened sun, UofHouston form	1	1	1	1
REFDAY	Day of the year chosen for the design point, day 1 is Jan 1st.	81	81	81	81

Variable	Description	Surround Field – Base Case	Surround Field – High Temp	North Field – Base Case	North Field – High Temp
	=81 March 21, equinox				
REFTIM	Design point hour on or past noon on the REFDAY	0	0	0	0
REFSOL	Design point insolation (kw/m2)	0.95	0.95	0.95	0.95
ASTART	Maximum sun angle (deg) w/ respect to vertical at which plant will begin operation	75	75	75	75
IATM	Atmospheric attenuation model =0 25 km visibility (Barstow) =1 5 kim visibility (Barstow) =2 user defined (see below)	0	0	0	0
FIELD					
NAZM	Number of zone divisions azimuthally around tower	12	12	12	12
NRAD	Number of zone divisions in the radial direction from the tower	12	12	12	12
RADMIN RADMAX	Min and Max radial position of heliostats, in units normalized to tower height (THT in REC)	0.75 7.5	0.75 7.5	0.75 7.5	0.75 7.5
INORTH	Control parameter for surround vs north-only field =0, surround field w/ equally spaced azimuthal zones =1 finer zoning of the north part of the field set my AMAXN	0	0	1	1
AMAXN	Maximum angle (deg) from north-south axis for north field zoning (INORTH=1)	N/A	N/A	82.5	82.5
ILAY	Heliostat layout patter, =0 radial stagger (only option)	0	0	0	0
IDENS	Heliostat density (1,2,4 based on Uhouston results) =1 high reflectivity (~0.9) rectangular helios	1	1	1	1
IUSERF	Parameter for field option for initial performance calc =0 circular field =1 code defined north biased field =2 user defined field specified zone by zone =3 user defined field specified by individual helio coordinates	0	0	0	0
NLAND	Parameter specifying land constrained field parameters, =0 no land constraint	0	0	0	0
FLAND(K,L)	Fraction of the area of the (K,L) zone that can have helios (can also be used for field trim or partial cloud cover)	156*1.0	156*1.0	156*1.0	156*1.0
IROTFL	Heliostat rotation, =0 stationary field	0	0	0	0
HSTAT					
WM HM	Width and Height in meters of heliostat, including edges supports/structures	9.91 9.93	9.91 9.93	9.91 9.93	9.91 9.93
ICPANL	Parameter for optional specification of location of individual cant panels	0	0	0	0
DENSMR	Ratio of mirror area to total area (WMxHM)	0.97	0.97	0.97	0.97

Variable	Description	Surround Field – Base Case	Surround Field – High Temp	North Field – Base Case	North Field – High Temp
IROUND	Heliostat shape parameter, =0 rectangular, =1 round	0	0	0	0
RMIRL	Average reflectivity of the mirrored surface	0.892	0.892	0.892	0.892
SIGEL, SIGAZ	Standard deviation in radians of the normal error distributions of the elevation and azimuth angles	0.00075 0.00075	0.00075 0.00075	0.00075 0.00075	0.00075 0.00075
SIGSX, SIGSY	Standard deviations (rad) in the normal error distributions of the hlio reflective surface normal	0.001 0.001	0.001 0.001	0.001 0.001	0.001 0.001
SIGTX, SIGTY	Standard deviations (rad) of the normal error distributions of reflected vector	0.000 0.000	0.000 0.000	0.000 0.000	0.000 0.000
ICANT	Canting parameter =0 no canting =-1 individual on-axis cant at a distance equal to slant range =1 user defined on-axis canting, specified by RCANT	1	1	1	1
NCANTX NCANTY	Number of submirror panels in a canted heliostat	2 8	2 8	2 8	2 8
RCANT(K)	Focal length, in units of tower heights (THT) at which all heliostats in the Kth radial zones are canted, can be used to define one canting for whole field	1	1	1	1
XFOCUS YFOCUS	Focusing of mirror panels or subpanels (1 indicates focusing in that direction)	1 1	1 1	1 1	1 1
IFOCUS	Types of focusing =0 individual focus w/ focal length equal to the slant range =1 user defined focal length determined, can be used to set focus for whole field	1	1	1	1
XFOCAL(K) YFOCAL(K)	User defined focal lengths for K radial zone, units of tower heights	13*6.00 13*6.00	13*6.00 13*6.00	13*6.00 13*6.00	13*6.00 13*6.00
INDC	Control parameter for more accurate heliostat images during performance only calcs, =0 for regular images	0	0	0	0
ISB	Parameter for overlapping of shadowing and blocking =0 no overlap, most conservative as shading and blocking losses are max =1 complete overlap, lower bound on shading and blocking losses	0	0	0	0
REC					
THT	Tower height, meters of the center of the external receiver or cavity above heliostat pivot point	175	175	175	175
TOWL TOWD	Shadow cast by the tower and receiver, TOWL meters tall and diameter of TOWD	175 10	175 10	175 10	175 10
IREC	Receiver type =0 vertical cylindrical external receiver =1 cavity w/ elliptical cross section =2 cavity w/ rectangular cross section =3 elliptical shape flat plate receiver =4 rectangular shape flat plate receiver	0	0	2	2
W	Diameter in meters of external receiver	16	16	16	16
H	Height in meters of external receiver	16	16	16	16

Variable	Description	Surround Field – Base Case	Surround Field – High Temp	North Field – Base Case	North Field – High Temp
RRECL	Fraction of incident power absorbed by the receiver before radiation and convection losses but after receiver reflection loss	0.94	0.94	0.94	0.94
IAUTOP	Aiming strategy, =0 single aim point at center of receiver =1, 1-d aiming strategy, =2, 2-d aiming strategy	1	1	2	2
NUMCAV	Number of apertures in a cavity receiver	N/A	N/A	1	1
RELV(I) RAZM(I)	Orientation of the outward normal vector for the Ith aperture RELV is the polar angle (=90 for vertical, >90 for down facing) RAZM is the azimuthal angle in degrees (=0 for south facing, =90 for west facing, =180 for north facing, =270 for east facing)	N/A	N/A	4*90 180, 270, 0, 90	4*90 180, 270, 0, 90
RX(I) RY(I)	Dimensions in meters of the Ith cavity aperture or flat plate receiver, RX is horizontal	N/A	N/A	4*6 4*6	4*6 4*6
RWCAV(I)	Ratio of the radius of the vertical cylindrical heat absorbing surface centered on the Ith aperture to the radius (W/2) of the receiver. Greater RWCAV means greater heat exchanger area.	N/A	N/A	4*1.0	4*1.0
NLFLUX					
IFLX	Perform flux calculation. =0 no flux calculation =1 flux calc desired	1	1	1	1
IFXOUT(I,J)	Specifying what time/day flux calc is desired	144*0	144*0	144*0	144*0
IFLAUT	Specifying surface of flux points, 4 is auto generate	4	4	4	4
NXFLX	Number of divisions for flux points	4	1	4	1
ICAVF(I)	Aperture(s) through which incident light can reach flux surface	1,0,0,0	1,0,0,0	1,0,0,0	1,0,0,0
NFLXMX FAZMIN FAZMAX	Points on receiver tested during field layout to check if FLXLIM exceeded	4 0 270	1 180 180	4 0 270	1 180 180
FLXLIM(I)	Maximum allowed flux on the receiver in W/m2	(1,2,3,4)=1x10^6	(1)=1x10^6	(1,2,3,4)=1x10^6	(1)=1x10^6
NLEFF					
REFLP	Reference pipe length (m) for calculating piping insulation losses	170	170	170	170
REFPIP	Fraction of REFRC*REFTHP delivered to storage and EPGS after piping losses	0.99	0.981	0.99	0.981
FPLH	Factor multiplying tower height to give total hot piping run in single module	2.6	2.6	2.6	2.6
FPLC	Factor multiplying tower height to give total cold piping run in single module	2.6	2.6	2.6	2.6
ITHEL	Design point thermal/electric conversion efficiency (=0 for constant efficiency)	0	0	0	0
ETAREF	Design point thermal/electric conversion efficiency	0.4183	0.5	0.4183	0.5

Variable	Description	Surround Field – Base Case	Surround Field – High Temp	North Field – Base Case	North Field – High Temp
FEFF	Fraction of design point efficiency describing average off-design operation	0.90	0.90	0.90	0.90
REFPRL	Design point parasitic load, fraction of gross electrical output	0.103	0.103	0.103	0.103
FSP	Fraction of design point parasitic load required for operation from storage	0.66	0.66	0.66	0.66
FEP	Fraction of design point parasitic load for operation electrical generating pumps	0	0	0	0
EFFSTR	Round Trip Efficiency through storage	0.985	0.95	0.985	0.95
PF	Plant factor, fraction of the year in which plant will come online	0.90	0.90	0.90	0.90
SMULT	Solar multiple at design point	1.8	1.8	1.8	1.8
IPH	Industrial process heat run instead of electrical plant =0 electrical plant, ~=0 industrial process heat	0	0	0	0
REFRC1 ,2 ,3	Coefficients for calculating thermal losses based on receiver area. 1 is for rad, others for conv losses (default values are for IREC=0 ONLY)	16403 460 0	20832 506 0	16403 7631 5077	20832 8400 5589
IRADFL	Which rad/conv loss algorithm to use (=1 for DELSOL2)	0	0	0	0
PARL1 PARL2 PARL3 PARL4 PARL5 PARL6 PARL7 PARL8 PARL9 PARL10	Nonoperation parasitic loss algorithm coefficients	0.5 0.103 0.5 0.103 0.5 0.008 0.5 0.008 0.18 0.009	0.5 0.103 0.5 0.103 0.5 0.008 0.5 0.008 0.18 0.009	0.5 0.103 0.5 0.103 0.5 0.008 0.5 0.008 0.18 0.009	0.5 0.103 0.5 0.103 0.5 0.008 0.5 0.008 0.18 0.009
TPRE TSTART	Time in hours spend every morning and again every evening for parasitic losses of (pre)startup/(post)shutdown	1 1	1 1	1 1	1 1
OPT					
IHOPT	Optimizing heliostat densities =0 no heliostat density optimization, field boundary is	0	0	0	0
NUMTHT THTST THTEND	THT will be varied by NUMTHT number of discrete equally spaced values from THTST to THTEND. If NUMTHT=1, then no optimization	20 75 400	20 75 400	20 75 400	20 75 400
NUMREC WST WEND	W is varied by NUMREC (equally spaced) from WST to WEND	10 8 26	10 10 5 5 40 40	10 8 26	10 10 5 5 40 40
NUMHTW HTWST HTWEND	Vary receiver H/W ratio (equally spaced) from HTWST to HTWEND, IOPTUM=1 for external receivers	10 0.5 2.0	10 10	10 0.5 2.0	10 10

Variable	Description	Surround Field – Base Case	Surround Field – High Temp	North Field – Base Case	North Field – High Temp
IOPTUM		1	5 0.5 40 2.0 2 1	2	5 0.5 40 2.0 2 1
RYTRX et al	RYTRX is ratio RY(1)/RX(1) assumed to be the same for all apertures or flat plates RX@TRX is ratio RX(2)/RX(1), etc	1	1	1	1
NUMOPT POPTMN POPTMX	Equally spaced net electrical power design power levels in watts (cost models not accurate below 10^7 watts)	1 $100x10^6$ $100x10^6$	1 $100x10^6$ $100x10^6$	1 $100x10^6$ $100x10^6$	1 $100x10^6$ $100x10^6$
NLAND et al	Land constrained field parameters =0, no land constraint	0	0	0	0
SMULT	Solar Multiple	1.8	1.8	1.8	1.8
IPLFL(I)	Output written to Unit 30 for I power level (for =1)	(1)=1	(1)=1	(1)=1	(1)=1
IPROPT	Output of zone by zone field buildup =0 output suppressed, =1 LARGE amount of output, -1 limited output ("strongly recommended")	-1	-1	-1	-1
IHOPTP	Detailed output of helio density optimization (=0, output suppressed)	0	0	0	0
IOTAPE	Write results to Unit 30 (=0 no writing, =1 writing)	1	1	1	1
IRERUN	Automatically rerun detailed performance calculation of an optimized system (=0 no rerun, =1 rerun for IPLFL and TDESP)	1	1	1	1
IALL	=0 smart search, =1 all possible combos	0	0	0	0
ISTR	Storage optimization =0 no optimization, maximum size used ~=0 optimum storage size determined (see below	0	0	0	0
NSTR	Number of storage sizes to consider for optimization	1	1	1	1
NLCOST					
CH	Cost of heliostats including wiring $/m2 mirror surface	120	120	120	120
CL	Cost of land including site prep $/m2	0.62	0.62	0.62	0.62
CWR CWDR CWDA	Wiring cost parameters	0.03077 15.0 9.0	0.03077 15.0 9.0	0.03077 15.0 9.0	0.03077 15.0 9.0
ITHT	Tower cost parameter, =0 cost based on Sandia studies for concrete and steel towers	0	0	0	0
CTOW1 CTOW2 CTOW3 XTOW	Tower cost parameters	782320 0.0113 1090250 0.00879	782320 0.0113 1090250 0.00879	782320 0.0113 1090250 0.00879	782320 0.0113 1090250 0.00879
CREC1 ARECRF XREC	Receiver cost parameters	23000000 758 0.8	23000000 758 0.8	23000000 758 0.8	23000000 758 0.8

Variable	Description	Surround Field – Base Case	Surround Field – High Temp	North Field – Base Case	North Field – High Temp
CRPREF TRPREF SMRP PRPREF XRP	Receiver/tower pump cost parameters	2100000 170.0 1.5 260000000 0.85	2100000 170.0 1.5 260000000 0.85	2100000 170.0 1.5 260000000 0.85	2100000 170.0 1.5 260000000 0.85
CSPREF PSPREF XSP	Storage pump cost parameters	470000 300000000 0.15	470000 300000000 0.15	470000 300000000 0.15	470000 300000000 0.15
CHPREF CCPREF SMPI PRIREF XPI	Piping cost parameters	28400 0.0 1.5 260000000 1.06	28400 0.0 1.5 260000000 1.06	28400 0.0 1.5 260000000 1.06	28400 0.0 1.5 260000000 1.06
CSTREF CSTRMD VSTREF ESTREF XST VMAX EMPTY3	Storage cost parameters	9700000 6800000 3740.0 688000000 0.6 12300 0.0	9700000 6800000 3740.0 688000000 0.6 12300 0.0	9700000 6800000 3740.0 688000000 0.6 12300 0.0	9700000 6800000 3740.0 688000000 0.6 12300 0.0
ICHE	Heat exchanger cost parameter, =0 cost scales w/ thermal power	0	0	0	0
CHEREF PHEREF XHEP	Heat exchanger cost parameters scaling w/ thermal power	1500000 173000000 0.8	1500000 173000000 0.8	1500000 173000000 0.8	1500000 173000000 0.8
CEGREF PEGREF XEPGS	EPGS cost parameters	37500000 112000000 0.8	37500000 112000000 0.8	37500000 112000000 0.8	37500000 112000000 0.8
CFIXED	Unusual fixed costs (other fixed costs are included)	0	0	0	0
ICKN	Sodium to salt heat exchanger (=0 not included)	0	0	0	0
NLECON					
CONT	Contingencies, fraction of total capital cost	0.12	0.12	0.12	0.12
SPTS	Spare parts investment, fraction of capital cost	0.01	0.01	0.01	0.01
EXT	Distributable and indirect charges, fraction of total capital cost	0.16	0.16	0.16	0.16
ESC	Yearly capital escalation rate, fraction	0	0	0	0
RINF	Yearly general inflation rate, fraction	0	0	0	0
NYTCON	Years to beginning of construction from year in which capital cost was made	0	0	0	0
AFDC	Allowed funds during construction to cover interest charges, expressed as fraction of the total capital cost	0.0318	0.0318	0.0318	0.0318
IFCR	Parameter to determine FCR (~=0, code calculates)	0	0	0	0
FCR	Fixed charge rate, fraction	0.0615	0.0615	0.0615	0.0615
DISRT	Discount rate, fraction	0.0315	0.0315	0.0315	0.0315
PTI	Property tax and insurance rate, fraction of cap cost	0.01	0.01	0.01	0.01

Variable	Description	Surround Field – Base Case	Surround Field – High Temp	North Field – Base Case	North Field – High Temp
TC	Investment tax credit, fraction of total investment	0.10	0.10	0.10	0.10
TR	Income tax rate, fraction	0.48	0.48	0.48	0.48
FDEBT	Fraction of debt financing	0.5431	0.5431	0.5431	0.5431
RDEBT	Debt cost, interest rate for borrowed funds, fraction	0.11	0.11	0.11	0.11
ROE	Before tax return on equity, fraction	0.15	0.15	0.15	0.15
IDEP	Depreciation schedule parameter =1 straight line method =2 sum of years digits method	2	2	2	2
NDEP	Depreciation period in years	24	24	24	24
NYOP	Operating life in years	30	30	30	30
RHOM	Heliostat operating and maintenance charge, fraction of field related capital costs	0.015	0.015	0.015	0.015
RNHOM	Balance of plant O&M charge, fraction of non-field related capital costs	0.015	0.015	0.015	0.015

APPENDIX B: ADDITIONAL DELSOL OUTPUTS

Table B. 1. DELSOL Outputs - Total Mirror Area.

Surround Field – Base Case	9.18×10^5 m^2
Surround Field – High Temperature Case	7.91×10^5 m^2
North Field – Base Case	8.68×10^5 m^2
North Field – High Temperature Case	7.73×10^5 m^2

Optical Efficiency Matrices

The following include the 0.893 heliostat reflectivity and 0.94 receiver absorptivity values; the receiver absorptivity was removed before entering the matrix into SOLERGY.

Table B. 2. Optical Efficiency Matrix - Surround Field Base Case.

		Elevation Angles						
		0°	5°	15°	25°	45°	65°	89.5°
Azimuth Angles	0°	0.000	0.253	0.427	0.520	0.578	0.592	0.603
	30°	0.000	0.253	0.426	0.517	0.576	0.590	0.603
	60°	0.000	0.246	0.417	0.508	0.569	0.587	0.603
	75°	0.000	0.281	0.420	0.505	0.564	0.584	0.603
	90°	0.000	0.233	0.404	0.496	0.560	0.582	0.603
	110°	0.000	0.267	0.405	0.491	0.554	0.578	0.603
	130°	0.000	0.271	0.400	0.486	0.550	0.575	0.603

Table B. 3. Optical Efficiency Matrix – Surround Field High Temperature Case.

		Elevation Angles:						
		0°	5°	15°	25°	45°	65°	89.5°
Azimuth Angles	0°	0.000	0.257	0.426	0.518	0.576	0.592	0.607
	30°	0.000	0.257	0.425	0.516	0.574	0.591	0.607
	60°	0.000	0.253	0.420	0.510	0.570	0.589	0.607
	75°	0.000	0.285	0.426	0.509	0.567	0.587	0.607
	90°	0.000	0.244	0.411	0.502	0.564	0.586	0.607
	110°	0.000	0.277	0.416	0.500	0.560	0.583	0.607
	130°	0.000	0.278	0.413	0.497	0.558	0.581	0.607

Table B. 4. Optical Efficiency Matrix - North Field Base Case.

		Elevation Angles:						
		0°	5°	15°	25°	45°	65°	89.5°
Azimuth Angles	0°	0.000	0.288	0.500	0.590	0.626	0.602	0.553
	30°	0.000	0.282	0.476	0.572	0.612	0.592	0.553
	60°	0.000	0.272	0.438	0.530	0.572	0.567	0.553
	75°	0.000	0.270	0.409	0.497	0.545	0.550	0.552
	90°	0.000	0.250	0.380	0.461	0.516	0.532	0.552
	110°	0.000	0.232	0.336	0.410	0.477	0.509	0.552
	130°	0.000	0.198	0.295	0.366	0.441	0.490	0.551

Table B. 5. Optical Efficiency Matrix - North Field High Temperature Case.

		Elevation Angles:						
		0°	5°	15°	25°	45°	65°	89.5°
Azimuth Angles	0°	0.000	0.299	0.489	0.569	0.600	0.576	0.533
	30°	0.000	0.281	0.461	0.552	0.587	0.568	0.533
	60°	0.000	0.271	0.428	0.511	0.549	0.544	0.532
	75°	0.000	0.258	0.400	0.480	0.524	0.529	0.532
	90°	0.000	0.248	0.370	0.445	0.497	0.513	0.531
	110°	0.000	0.226	0.328	0.398	0.460	0.492	0.531
	130°	0.000	0.197	0.293	0.359	0.428	0.474	0.531

APPENDIX C: DETAILED SOLERGY INPUTS

Variable	Description	Surround Field – Base Case	Surround Field – High Temp	North Field – Base Case	North Field – High Temp
NMLGEN					
DELT	Time step in hours	0.25	0.25	0.25	0.25
IFOUT	Julian dates of forced outage days	0	0	0	0
ISCHED	Julian dates of scheduled outage days	0	0	0	0
NMLLOC					
ALAT	Local latitude (degrees)	34.897	34.897	34.897	34.897
ALONG	Local longitude (degrees)	117.022	117.022	117.022	117.022
ZONE	Local international time zone	8	8	8	8
IFLAGP	Detailed output of sun position	0	0	0	0
NMLCOEF					
NX	Number of rows in FR array (number of EL angles)	7	7	7	7
NY	Number of columns in the FR array (number of AZ angles)	7	7	7	7
AZR	Azimuth Angles (degrees) (consistent w/ DELSOL)	0, 30, 60, 75, 90, 110, 130	0, 30, 60, 75, 90, 110, 130	0, 30, 60, 75, 90, 110, 130	0, 30, 60, 75, 90, 110, 130
ELR	Elevation Angles (degrees) (flipped from DELSOL)	0, 5, 15, 25, 45, 65, 89.5	0, 5, 15, 25, 45, 65, 89.5	0, 5, 15, 25, 45, 65, 89.5	0, 5, 15, 25, 45, 65, 89.5
FR	Field efficiency matrix	(See **Appendix B: Additional DELSOL** Outputs)			
NMLCOLF					
FS	Collector field reflective area	918000	791000	868000	773000
TLIML	Lower collector field operating limit (°F)	0	0	0	0
TLIMU	Upper collector field operating limit (°F)	120	120	120	120
WSLIM	Maximum wind speed for field operation (m/s)	17.9	17.9	17.9	17.9
ELIM	Minimum solar elevation angle for collector field operation (degrees)	0	0	0	0
RFLCTY	Heliostat reflectivity, if not included in FR	1.0	1.0	1.0	1.0
NEFWS	Number of elements in the wind speed efficiency array	8	8	8	8
WSX	Wind speed values for spline fit (m/s)	0, 2, 4, 6, 8, 10, 12, 13.4	0, 2, 4, 6, 8, 10, 12, 13.4	0, 2, 4, 6, 8, 10, 12, 13.4	0, 2, 4, 6, 8, 10, 12, 13.4
WSEF	Wind speed efficiency factor	8*1.0	8*1.0	8*1.0	8*1.0
NMLRCVR					
EPS	Receiver absorptivity	0.94	0.94	0.94	0.94
RS	Receiver thermal rating (MW_t)	430.2	360	430.2	360

Variable	Description	Surround Field – Base Case	Surround Field – High Temp	North Field – Base Case	North Field – High Temp
ALPHAR	Receiver cool down parameter ($hours^{-1}$)	0.2	0.2	0.2	0.2
TREQD	Time delay for receiver startup (hours)	0.75	0.75	0.75	0.75
EREQD	Energy required for receiver startup (MW_th)	0	0	0	0
RMF	Receiver minimum flow fraction	0.16	0.16	0.16	0.16
IFILL	Receiver door flag	1	1	1	1
PLXLR	(not listed in Solergy Manual) thermal loss, in MWt, during operation	19.128	16	19.128	16
EXFAC	Fraction of insolation that is unusable	0	0	0	0
NMLPIPE					
NXLP	Number of elements in temperature vector	9	9	9	9
TXLP	Vector of ambient temperature points for spline fit, in ascending order (°C)	-22, -4, 14, 32, 50, 68, 86, 104, 122	-22, -4, 14, 32, 50, 68, 86, 104, 122	-22, -4, 14, 32, 50, 68, 86, 104, 122	-22, -4, 14, 32, 50, 68, 86, 104, 122
YXLP	Vector of corresponding loss coefficients	0.00034730.0003393 0.0003313 0.0003232 0.0003152 0.0003071 0.0002991 0.0002911 0.000283	0.0006599 0.0006447 0.0006295 0.0006141 0.0005989 0.0005835 0.0005683 0.0005531 0.000538	0.00034730.0003393 0.0003313 0.0003232 0.0003152 0.0003071 0.0002991 0.0002911 0.000283	0.0006599 0.0006447 0.0006295 0.0006141 0.0005989 0.0005835 0.0005683 0.0005531 0.000538
NMLSTRG					
PTSMAX	Maximum charging rate (MWt)	430.2	360	430.2	360
PFSMAX	Maximum discharge rate (MWt)	239	200	239	200
PTSMIN	Minimum charging rate (MWt)	0	0	0	0
PFSMIN	Minimum discharge rate (MWt)	0	0	0	0
EMAX	Maximum value of the stored energy (MWthr)	1434	1200	1434	1200
EMIN	Minimum value of the stored energy (MWthr)	0	0	0	0
ES	Energy in storage (MWthr)	0	0	0	0
A(*)	Thermocline degradation coefficients	3*0.0	3*0.0	3*0.0	3*0.0
CLF	Charging loss factor (MW)	0	0	0	0
DLF	Discharging loss factor (MW)	0.33	0.65	0.33	0.65
TNKLF	Tankage loss factor (MWt or hr)	0.33	0.65	0.33	0.65
LS	Storage flag	1	1	1	1
REFPC	Reference power for heat exchanger thermal losses (MWt)	239	200	239	200
TSTCR	Minimum time delay for storage charging startup (hr)	0	0	0	0
ESTCR	Energy penalty for storage charging startup (MWthr)	0	0	0	0

Variable	Description	Surround Field – Base Case	Surround Field – High Temp	North Field – Base Case	North Field – High Temp
TSTDR	Minimum time delay for storage discharging startup (hr)	0	0	0	0
ESTDR	Energy penalty for storage discharging startup (MWthr)	0	0	0	0
PWARMC	Maximum charging rate during charging startup (MWt)	430.2	360	430.2	360
PWARMD	Maximum extraction rate during extraction startup (MWt)	30	30	30	30
NMLTRBN					
TBHWS	Time between hot and warm startup (hr)	12	12	12	12
TBWCS	Time between warm and cold startup (hr)	60	69	60	69
SDH	Hot turbine sync delay (hr)	0.25	0.25	0.25	0.25
SDW	Warm turbine sync delay (hr)	1.0	1.0	1.0	1.0
SDC	Cold turbine sync delay (hr)	1.8	1.8	1.8	1.8
RDH	Hot turbine ramp delay (hr)	0.4	0.4	0.4	0.4
RDW	Warm turbine ramp delay (hr)	1.7	1.7	1.7	1.7
RDC	Cold turbine ramp delay (hr)	2.7	2.7	2.7	2.7
TPFSL	Thermal power for rated turbine operation (MWt)	239	200	239	200
TMFS	Minimum turbine flow fraction	0.3	0.3	0.3	0.3
ESMIN1	Minimum storage energy level for turbine start, peak period, receiver operating (MWthr)	57.36	48	57.36	48
ESMIN2	Minimum storage energy level for turbine start, peak period, receiver not operating (MWthr)	239	200	239	200
ESMAX1	Storage level at which turbine must be started, receiver operating (MWthr)	57.36	48	57.36	48
ESMAX2	Storage level at which turbine must be started, receiver not operating (MWthr)	1434	1200	1434	1200
NREPSS	Number of rows in FEPSS matrix (no. of wetbulb temperatures)	6	6	6	6
NCEPSS	Number of columns in FEPSS matrix (no. of fraction of rated power)	4	4	4	4
REPSS	Row vector of fractions of rated power for bicubic spline, ascending order	0.2907, 0.5239, 0.7563, 1.0	0.2907, 0.5239, 0.7563, 1.0	0.2907, 0.5239, 0.7563, 1.0	0.2907, 0.5239, 0.7563, 1.0
CEPSS	Column vector of wet bulb temperature values (°C) for bicubic spline, ascending order	30, 40, 50, 60, 70, 80	30, 40, 50, 60, 70, 80	30, 40, 50, 60, 70, 80	30, 40, 50, 60, 70, 80
FEPSS	Matrix values for thermal to electric conversion efficiency (order important)	6*0.3598, 6*0.3992, 6*0.4148, 6*0.4183	6*0.4301 6*0.4772 6*0.4958 6*0.5	6*0.3598, 6*0.3992, 6*0.4148, 6*0.4183	6*0.4301 6*0.4772 6*0.4958 6*0.5
DISPATCH					
IDISP	Dispatch strategy selection 0=GONOGO, 1=MAXOUT	0	0	0	0

Variable	Description	Surround Field – Base Case	Surround Field – High Temp	North Field – Base Case	North Field – High Temp
TSTUR	Estimated average time for turbine startup (hours)	1.25	1.25	1.25	1.25
PSTFR	Estimated fraction of rated turbine power output during turbine startup	0.5	0.5	0.5	0.5
IDF1, IDF2	Print dispatch strategy trace (MAXOUT options) to output file DISPAT.TRC from day IDF1 to IDF2	400 0	400 0	400 0	400 0
PRNTOUT					
MFLAG	Output detail print flag 0=minimal output, annual summaries printed 1=in addition to previous, daily summaries printed 2=in addition to previous, power flow and storage for each time step is printed 3=in addition to previous, collector field efficiency and power to the receiver at each time step is printed 4=in addition to previous, input data from weather file is printed	3	3	3	3
NDAF	First day to be printed with MFLAG information	1	1	1	1
NDAL	Last day of the run	365	365	365	365
PRSTIC					
PA(1)	Power to run heliostat field (MW_e/m^2)	$5.22x10^{-7}$	$5.22x10^{-7}$	$5.22x10^{-7}$	$5.22x10^{-7}$
PA(2)	Power to stow/unstow heliostat field during 0.25 hr interval (MW_e/m^2)	$2.4x10^{-5}$	$2.4x10^{-5}$	$2.4x10^{-5}$	$2.4x10^{-5}$
PA(3) PA(4) PA(5) PA(6)	Cold salt pump curve-fit parameters	2.9675 2.058 6.6 0.0	2.9675 2.058 6.6 0.0	2.9675 2.058 6.6 0.0	2.9675 2.058 6.6 0.0
PA(7) PA(8)	Turbine plant curve-fit parameters	-1.0404 3.6395	-0.8861 7.2406	-1.0404 3.6395	-0.8861 7.2406
PA(9)	Solar Multiple	1.8	1.8	1.8	1.8
PA(10)	Hot salt pump power (MW_e), for SM<0.6	0.607	0.508	0.607	0.508
PA(11)	Hot salt pump power (MW_e), for 0.6<SM<1.1	0.607	0.508	0.607	0.508
PA(12)	Hot salt pump power (MW_e), for SM>1.1	0.607	0.508	0.607	0.508
PA(13)- PA(25)	PG&E cooler	1.65 0.21 0.239 0.275 0.537 0.608 1.04 1.35 1.18 0.728 0.469 0.293 0.251	1.65 0.21 0.239 0.275 0.537 0.608 1.04 1.35 1.18 0.728 0.469 0.293 0.251	1.65 0.21 0.239 0.275 0.537 0.608 1.04 1.35 1.18 0.728 0.469 0.293 0.251	1.65 0.21 0.239 0.275 0.537 0.608 1.04 1.35 1.18 0.728 0.469 0.293 0.251
PA(26)	Thermal losses, in MW_t, from receiver, during hold or	7.46	6.11	5.07	3.80

Variable	Description	Surround Field – Base Case	Surround Field – High Temp	North Field – Base Case	North Field – High Temp
	shutdown				
PA(27)	# of time steps allowed for receiver standby before shutdown of receiver	3.0	3.0	3.0	3.0
PA(28)	Baseline parasitics (MW_e), for overnight, weather, or forced outage	0.7	0.7	0.7	0.7
PA(29)	Baseline parasitics for scheduled outage (MW_e)	0.7	0.7	0.7	0.7
PA(30)	Shutdown Load	1.06	1.06	1.06	1.06

This page intentionally left blank.

APPENDIX D: ANNUAL SUMMARIES FROM SOLERGY

D.1 Surround Field – Base Case

```
   PLANT SUMMARY - DAYS 1 TO 365 YEAR 1985

EFFICIENCY         (MWHRS)             ENERGY LOSSES
         I-------------------------I    (MWHRS)
         I     TOTAL INSOLATION    I
         I       2485022.25        I
         I-------------------------I
                      V
         I-------------------------I OUTAGE LOSSES
   1.000 I     AVAILABLE ENERGY    I       0.00 (YEOUTAGE)
         I       2485022.25        I
         I-------------------------I
                      V
         I-------------------------I FIELD LOSSES
   1.000 I    REDIRECTED ENERGY    I       0.00 REFLECTIVITY LOSS
   0.562 I       1395364.37        I 1089657.87 COSINE, SHADOWING, BLOCKING,
         I-------------------------I              SPILLAGE, TRANSMISION (AND OPERATION LIMITS=1069.54)
                      V
         I-------------------------I STORAGE FULL OR  CHARGING HX IN STARTUP
   0.949 I  RCVR INCIDENT ENERGY    I   71519.95 DEFOCUS HELIOSTATS (YSUPTR)
         I       1323844.37        I
         I-------------------------I
                      V
         I-------------------------I RECEIVER LOSSES
         I        RECEIVER         I   22394.31 RCVR MIN FLOW (YPLRMF)
         I     ABSORBED ENERGY     I   72566.19 SURPLUS ENERGY TO  RCVR (PTR TOO BIG) DEFOCUS HELIOSTATS (YSPTR)
   0.786 I                         I   73733.03 ABSORPTANCE
         I       1040015.37        I   63172.03 THERMAL LOSS (RADIATION AND CONVECTION)
         I-------------------------I   51963.31 RCVR STARTUP (YRSTRT)
                      V
         I-------------------------I PIPING LOSSES
   1.000 I    ENERGY TO STORAGE    I     403.87
         I       1039611.50        I
         I-------------------------I
                      V
         I-------------------------I STORAGE LOSSES
         I                         I       0.00 CHARGING HX START (YCSTRT)
         I        ENERGY TO        I       0.00 LOSS FROM CHARGING HX (YTPLDC)
   0.996 I         TURBINE*        I    2890.80 TANK LOSS (YTNKLOS)
         I       1035192.37        I       0.00 STEAM GENERATOR STARTUP (YESTRT)
         I-------------------------I    1527.82 LOSS FROM STEAM GEN (YTPLDD)
                      V                *    0.64 MWHRS IN STORAGE AT END OF DAY 365
                      V
         I-------------------------I EPGS LOSSES
   0.410 I      GROSS ENERGY       I   19809.19 TURBINE SYNC LOSS (YTSTRT)
         I        424241.88        I  591141.50 RANKINE LOSS (APPROX)
         I-------------------------I
                      V
         I-------------------------I AUXILIARY ENERGY
         I       NET ENERGY        I   15674.06 BALANCE OF PLANT (YBOPPAR)
   0.828 I         OUTPUT          I   13437.81 TURBINE PLANT (YTPPAR)
         I                         I   37847.21 SOLAR PLANT (YSPPAR)
         I       351150.69 MWHe    I    6131.98 OVERNIGHT  (YPMPAR)
         I-------------------------I       0.00 SHUTDOWN (YSDPAR)
   0.141                           (   73091.05 TOTAL AUX ENERGY (YPARN))

   0.141 OVERALL PLANT EFFICIENCY (TOTAL NET ELECTRICITY/TOTAL DNI ON FIELD)
```

D.2. Surround Field – High Temperature Case

```
  PLANT SUMMARY - DAYS 1 TO 365 YEAR 1985

EFFICIENCY        (MWHRS)           ENERGY LOSSES
        I-------------------------I   (MWHRS)
        I     TOTAL INSOLATION    I
        I       2141233.50        I
        I-------------------------I
                     V
        I-------------------------I OUTAGE LOSSES
  1.000 I     AVAILABLE ENERGY    I       0.00 (YEOUTAGE)
        I       2141233.50        I
        I-------------------------I
                     V
        I-------------------------I FIELD LOSSES
  1.000 I    REDIRECTED ENERGY    I       0.00 REFLECTIVITY LOSS
  0.564 I       1207618.25        I  933615.31 COSINE, SHADOWING, BLOCKING,
        I-------------------------I              SPILLAGE, TRANSMISION (AND OPERATION LIMITS= 922.35)
                     V
        I-------------------------I STORAGE FULL OR  CHARGING HX IN STARTUP
  0.944 I  RCVR INCIDENT ENERGY   I   67315.59 DEFOCUS HELIOSTATS (YSUPTR)
        I       1140302.62        I
        I-------------------------I
                     V
        I-------------------------I RECEIVER LOSSES
        I        RECEIVER         I   18127.87 RCVR MIN FLOW (YPLRMF)
        I     ABSORBED ENERGY     I   81026.86 SURPLUS ENERGY TO  RCVR (PTR TOO BIG) DEFOCUS HELIOSTATS (YSPTR)
  0.773 I                         I   62468.87 ABSORPTANCE
        I        880950.00        I   53174.08 THERMAL LOSS (RADIATION AND CONVECTION)
        I-------------------------I   44554.92 RCVR STARTUP (YRSTRT)
                     V
        I-------------------------I PIPING LOSSES
  0.999 I    ENERGY TO STORAGE    I     644.37
        I        880305.62        I
        I-------------------------I
                     V
        I-------------------------I STORAGE LOSSES
        I                         I       0.00 CHARGING HX START (YCSTRT)
        I        ENERGY TO        I       0.00 LOSS FROM CHARGING HX (YTPLDC)
  0.990 I         TURBINE*        I    5694.02 TANK LOSS (YTNKLOS)
        I        871607.44        I       0.00 STEAM GENERATOR STARTUP (YESTRT)
        I-------------------------I    3022.17 LOSS FROM STEAM GEN (YTPLDD)
                     V                 *  -17.06 MWHRS IN STORAGE AT END OF DAY 365
                     V
        I-------------------------I EPGS LOSSES
  0.490 I      GROSS ENERGY       I   16226.19 TURBINE SYNC LOSS (YTSTRT)
        I        427214.41        I  428166.19 RANKINE LOSS (APPROX)
        I-------------------------I
                     V
        I-------------------------I AUXILIARY ENERGY
        I       NET ENERGY        I   15712.35 BALANCE OF PLANT (YBOPPAR)
  0.792 I         OUTPUT          I   29174.86 TURBINE PLANT (YTPPAR)
        I                         I   37992.46 SOLAR PLANT (YSPPAR)
        I        338202.19 MWHe   I    6131.98 OVERNIGHT  (YPMPAR)
        I-------------------------I       0.00 SHUTDOWN (YSDPAR)
  0.158                            (  89011.72 TOTAL AUX ENERGY (YPARN))

  0.158 OVERALL PLANT EFFICIENCY (TOTAL NET ELECTRICITY/TOTAL DNI ON FIELD)
```

D.3. North Field – Base Case

```
  PLANT SUMMARY - DAYS 1 TO 365 YEAR 1985

EFFICIENCY        (MWHRS)           ENERGY LOSSES
        I-------------------------I   (MWHRS)
        I     TOTAL INSOLATION    I
        I       2349670.75        I
        I-------------------------I
                     V
        I-------------------------I OUTAGE LOSSES
  1.000 I     AVAILABLE ENERGY    I       0.00 (YEOUTAGE)
        I       2349670.75        I
        I-------------------------I
                     V
        I-------------------------I FIELD LOSSES
  1.000 I    REDIRECTED ENERGY    I       0.00 REFLECTIVITY LOSS
  0.565 I       1328699.75        I 1020970.94 COSINE, SHADOWING, BLOCKING,
        I-------------------------I              SPILLAGE, TRANSMISION (AND OPERATION LIMITS=1069.72)
                     V
        I-------------------------I STORAGE FULL OR  CHARGING HX IN STARTUP
  0.964 I  RCVR INCIDENT ENERGY   I   47553.93 DEFOCUS HELIOSTATS (YSUPTR)
        I       1281145.87        I
        I-------------------------I
                     V
        I-------------------------I RECEIVER LOSSES
        I        RECEIVER         I   23557.88 RCVR MIN FLOW (YPLRMF)
        I     ABSORBED ENERGY     I   52336.56 SURPLUS ENERGY TO  RCVR (PTR TOO BIG) DEFOCUS HELIOSTATS (YSPTR)
  0.797 I                         I   72315.09 ABSORPTANCE
        I       1020954.00        I   62213.24 THERMAL LOSS (RADIATION AND CONVECTION)
        I-------------------------I   49769.05 RCVR STARTUP (YRSTRT)
                     V
        I-------------------------I PIPING LOSSES
  1.000 I    ENERGY TO STORAGE    I     399.00
        I       1020555.00        I
        I-------------------------I
                     V
        I-------------------------I STORAGE LOSSES
        I                         I       0.00 CHARGING HX START (YCSTRT)
        I        ENERGY TO        I       0.00 LOSS FROM CHARGING HX (YTPLDC)
  0.996 I         TURBINE*        I    2890.80 TANK LOSS (YTNKLOS)
        I       1016169.87        I       0.00 STEAM GENERATOR STARTUP (YESTRT)
        I-------------------------I    1502.49 LOSS FROM STEAM GEN (YTPLDD)
                     V                *   -8.66 MWHRS IN STORAGE AT END OF DAY 365
                     V
        I-------------------------I EPGS LOSSES
  0.410 I      GROSS ENERGY       I   19904.08 TURBINE SYNC LOSS (YTSTRT)
        I        416234.66        I  580031.31 RANKINE LOSS (APPROX)
        I-------------------------I
                     V
        I-------------------------I AUXILIARY ENERGY
        I       NET ENERGY        I   15576.58 BALANCE OF PLANT (YBOPPAR)
  0.828 I         OUTPUT          I   13179.57 TURBINE PLANT (YTPPAR)
        I                         I   36710.68 SOLAR PLANT (YSPPAR)
        I        344635.78 MWHe   I    6131.98 OVERNIGHT  (YPMPAR)
        I-------------------------I       0.00 SHUTDOWN (YSDPAR)
  0.147                            (  71598.84 TOTAL AUX ENERGY (YPARN))

  0.147 OVERALL PLANT EFFICIENCY (TOTAL NET ELECTRICITY/TOTAL DNI ON FIELD)
```

D.4. North Field – High Temperature Case

```
  PLANT SUMMARY - DAYS 1 TO 365 YEAR 1985

EFFICIENCY        (MWHRS)            ENERGY LOSSES
        I-------------------------I   (MWHRS)
        I     TOTAL INSOLATION    I
        I       2092507.12        I
        I-------------------------I
                     V
        I-------------------------I OUTAGE LOSSES
  1.000 I     AVAILABLE ENERGY    I       0.00 (YEOUTAGE)
        I       2092507.12        I
        I-------------------------I
                     V
        I-------------------------I FIELD LOSSES
  1.000 I    REDIRECTED ENERGY    I       0.00 REFLECTIVITY LOSS
  0.545 I       1139419.00        I  953088.12 COSINE, SHADOWING, BLOCKING,
        I-------------------------I              SPILLAGE, TRANSMISION (AND OPERATION LIMITS= 916.82)
                     V
        I-------------------------I STORAGE FULL OR  CHARGING HX IN STARTUP
  0.960 I  RCVR INCIDENT ENERGY   I   45541.32 DEFOCUS HELIOSTATS (YSUPTR)
        I       1093877.62        I
        I-------------------------I
                     V
        I-------------------------I RECEIVER LOSSES
        I        RECEIVER         I   19316.25 RCVR MIN FLOW (YPLRMF)
        I     ABSORBED ENERGY     I   55102.34 SURPLUS ENERGY TO  RCVR (PTR TOO BIG) DEFOCUS HELIOSTATS (YSPTR)
  0.789 I                         I   61167.55 ABSORPTANCE
        I        863559.62        I   52234.29 THERMAL LOSS (RADIATION AND CONVECTION)
        I-------------------------I   42497.66 RCVR STARTUP (YRSTRT)
                     V
        I-------------------------I PIPING LOSSES
  0.999 I    ENERGY TO STORAGE    I     637.75
        I        862921.88        I
        I-------------------------I
                     V
        I-------------------------I STORAGE LOSSES
        I                         I       0.00 CHARGING HX START (YCSTRT)
        I        ENERGY TO        I       0.00 LOSS FROM CHARGING HX (YTPLDC)
  0.990 I         TURBINE*        I    5694.02 TANK LOSS (YTNKLOS)
        I        854276.94        I       0.00 STEAM GENERATOR STARTUP (YESTRT)
        I-------------------------I    2968.23 LOSS FROM STEAM GEN (YTPLDD)
                     V               *  -17.06 MWHRS IN STORAGE AT END OF DAY 365
                     V
        I-------------------------I EPGS LOSSES
  0.490 I      GROSS ENERGY       I   16402.66 TURBINE SYNC LOSS (YTSTRT)
        I        418453.75        I  419420.03 RANKINE LOSS (APPROX)
        I-------------------------I
                     V
        I-------------------------I AUXILIARY ENERGY
        I       NET ENERGY        I   15592.40 BALANCE OF PLANT (YBOPPAR)
  0.792 I         OUTPUT          I   28571.96 TURBINE PLANT (YTPPAR)
        I                         I   36845.19 SOLAR PLANT (YSPPAR)
        I        331311.75 MWHe   I    6131.98 OVERNIGHT  (YPMPAR)
        I-------------------------I       0.00 SHUTDOWN (YSDPAR)
  0.158                            (  87141.59 TOTAL AUX ENERGY (YPARN))

  0.158 OVERALL PLANT EFFICIENCY (TOTAL NET ELECTRICITY/TOTAL DNI ON FIELD)
```

DISTRIBUTION

1	MS 1127	David Gill	06123 (electronic copy)
1	MS 1127	Brian Ehrhart	06123 (electronic copy)
1	MS0899	Technical Library	9536 (electronic copy)

This page intentionally left blank.


Sandia National Laboratories